Summer 2011

Grid frequency and voltage support using photovoltaic systems with energy storage assist

Ravi Bhatt

Department:

GRID FREQUENCY AND VOLTAGE SUPPORT USING PHOTOVOLTAIC SYSTEMS WITH ENERGY STORAGE ASSIST

by

RAVI BHATT

A THESIS

Presented to the Faculty of the Graduate School of the

MISSOURI UNIVERSITY OF SCIENCE AND TECHNOLOGY

In Partial Fulfillment of the Requirements for the Degree

MASTER OF SCIENCE IN ELECTRICAL ENGINEERING

2011

Approved by

Dr. Badrul H. Chowdhury, Advisor
Dr. Jonathan Kimball
Dr. Mariesa L. Crow

ABSTRACT

An optimized operating scheme for a grid-connected community based photovoltaic (PV) system is described. The system can participate in grid ancillary services like frequency and voltage regulation functions based on the Smart Grid framework. The proposed model comprises of a PV plant with Li-ion batteries coupled to the grid by means of a three-phase inverter. A two-way communication between the PV plant and the grid is assumed. The PV/storage plant provides constant updates on its current kW/kVar capability and the grid transmits the demand for specific amounts of power and for specific lengths of time. The battery charging energy can originate from either the PV system or the grid depending on the prevailing energy prices. The batteries are discharged when two conditions are met: the grid requests energy from the community-based PV system and if the PV system itself fails to meet the requested kW or kVar demand. The PV plant and the battery storage are integrated with the grid with the help of dc-dc and dc-ac converters in such a way that bi-directional flow of active and reactive powers can be achieved. Controllers integrating energy sources respond to the received signals and attempt to fulfill the grid demand. The system response is almost instantaneous and thus can be very helpful in grid frequency and voltage support.

ACKNOWLEDGMENTS

I would like to express my deepest gratitude to my advisor, Dr. Badrul Chowdhury, for his supervision and encouragement throughout my Master's program. I appreciate all his contributions of time, ideas, and funding to make my M.S. experience productive and stimulating. I would like to specially mention his support, belief and willingness to help which kept me motivated and focused.

I would also like to extend my vote of thanks to my esteemed committee members Dr. Jonathan Kimball and Dr. Mariesa Crow for providing support and enthusiasm. If but not for their valuable timely advices and suggestions, this project would not had attained completion.

Special thanks also to all my graduate friends, Darshit Shah, Maigha Garg, Tu Nguyen and Anshuman Vaidya for sharing their knowledge and invaluable assistance. I would also like to thank my roommates and friends for being a constant source of support while away from family.

Lastly, and most importantly, I wish to thank my parents, Hemant Bhatt and Bhavna Bhatt and my brother, Mihir Bhatt. They raised me, supported me and loved me. To them I dedicate this thesis.

TABLE OF CONTENTS

LIST OF ILLUSTRATIONS

Figure Page

LIST OF TABLES

NOMENCLATURE

Symbol	Description
SOC	State of Charge
PV	Photovoltaic
P_{pv}	Power output of the PV panel
P_{batt}	Power at the battery terminal
P_{comm}	Active Power commanded by Grid
Q_{comm}	Reactive Power commanded by the grid
V_{dc}	Voltage at the DC bus
P_{grid}	Active Power at the Grid Interconnection Point
P_{ref}	Reference Power
DER	Distributed Energy Resource

1. INTRODUCTION

1.1 BACKGROUND

In today's dynamic world, electric utilities are facing challenges like rising energy demand, increasing fuel costs, aging assets, and pressure to adopt renewable portfolio standards, etc. [1]. Much of this can be tackled without compromising the overall performance and service quality of the grid supply. In recent years, the presence of photovoltaic (PV) generations on the utility grid is on the rise. With increase in PV penetration and the progress of the global PV market, there is a need to enable the PV systems with features which make them smart to create an effective business model. Further, by leveraging the Smart Grid technologies, and taking advantage of the distributed nature of PV, new opportunities to unlock value can be created. With the implementation of advanced energy storage techniques, effective two way communications and a robust demand response program, a grid-tied PV system can create additional value, primarily by enabling increased PV participation in grid support functions, such as frequency and voltage regulation.

PV generation has increased on a large scale especially in the US and Europe, with the largest plant rated at 60MW at Olmedilla, Spain [2]. If proper control technique is available, such large plants can work hand in hand with the grid to increase system reliability. The ultimate goal of any power system is to maintain a balance between demand and supply of active and reactive power at any given point in time. Any difference between the demanded and the generated quantities directly impacts the system frequency and voltage. The traditional approach to achieve frequency regulation is to use fossil fuel and hydro reserves to generate electrical energy on demand [3]; while

the general approach to achieve voltage regulation is to use generator var reserves, shunt capacitors, and var compensators when needed.

This thesis discusses a method to provide active and reactive power compensation to the grid to participate in frequency and voltage regulation functions. Multifunction approach increases the utilization factor and improves the quality of the grid supply [4]. Energy storage systems are promising technologies which may work symbiotically with PV systems to regulate frequency and voltage.

1.2 PROPOSED APPROACH

In conventional power systems, the grid provides ancillary services such as frequency regulation, voltage support, spinning reserves etc. These services are typically not free, i.e., generators are paid for ancillary support in regions which have such a market [5]. As shown in Fig. 1.1 the objective is to propose a power management system which would tap the future energy markets for frequency and voltage regulation and create an enhanced value for PV systems.

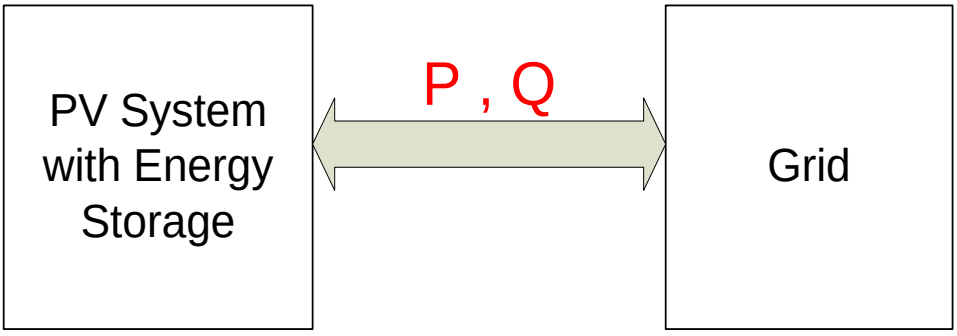

Figure 1.1 Grid connected PV systems for Regulation

In this thesis, control over the active and reactive power output of a PV system is proposed. Three energy sources, namely, a PV array, battery storage and the grid are integrated together by means of three converters and controlled by three controllers to provide bi-directional flow of active and reactive power. With the suggested technique, PV systems can deliver a variable amount of active and reactive power based on the amount demanded from the grid. This enables grid frequency and voltage support. Thus, frequency and voltage management may be possible even under islanded operating conditions.

1.3 CONTRIBUTIONS OF THE THESIS

The main contributions of this thesis are:

- Development of the power management scheme between a community-based PV system, an energy storage system and the grid that provides frequency and voltage support to the grid.
- Development and design of the power stages such as boost converter, bi-directional dc-dc converter and an inverter
- Development of the stable asynchronous control scheme for managing the power flow between PV array, battery and the grid.
- Validation of the proposed scheme by simulating the system under various scenarios.

1.4 THESIS ORGANIZATION

This thesis is organized into six sections. Section 1 provides a general introduction and proposed scheme for the regulation. The system is participating in an ancillary support mode.

Section 2 describes the background for the research. It covers literature review and provides an overview on similar work reported in the pertinent literature. It sheds light on existing power management systems with renewable energy sources.

Section 3 presents methods of determining the regulation capability of the system. It explains the factors contributing towards systems ability to provide active and reactive power. It also proposes a unique way of achieving the regulation and increasing the grid friendliness.

Section 4 introduces the system, the topology used and the associated control. It explains the modeling of the three energy sources in detail and also discusses their control under various scenarios.

Section 5 presents the simulation results. The system is tested under different scenarios to show that operation is instantaneous in response to the commanded signals.

Section 6 presents the conclusions. Recommendations for future research are also discussed in this section.

2. BACKGROUND

Renewable energy resources for power generation have been one of the most widely discussed topics in the technical literature for power engineering for more than two decades now. There has been a rising concern for depleting fossil fuel sources, which has given a further boost to research in the field of renewable energy. Characteristics like, non-polluting, low maintenance, increased lifetime, and noise-free operation have led to an increased interest in renewable resources. This idea, along with the advancement in power electronics, has led to the widespread harvesting of the freely available resources like wind and solar. Further, the statutory incentives applicable through federal laws, have further given a momentum to the implementation of renewable sources for power generation.

There is an extensive literature available that advocates the use of ancillary services market in bridging the gap between the grid and DG resources [6-10]. References [6, 8] discuss the concept of 'unbundled or ancillary' services. It has been shown that active and non-active power control can increase grid friendliness by providing ancillary services like voltage control, frequency regulation, load following, spinning reserve, supplemental reserve, backup supply and peak shaving. Table 2.1 summarizes the current ancillary service products.

Technical and economic aspects, along-with dependability, determine the benefit drawn from ancillary services. Further, these services can be categorized based on the maximum benefit they would entail either to the grid, DG owner or both. The availability

Table 2.1 P-Q capabilities for ancillary services [7]

Ancillary Services	Active Power P	Reactive Power Q
Frequency Control	✓	✗
Voltage Control, Congestion Management	☑	✓
Black start	✓	✓
Islanded Operation	✓	✓
Fault ride-through	☑	✓

✓ Required

☑ Also possible

✗ Not possible

of high energy density storage devices and advancement in semiconductors, have given a new edge to the usage of these services [6, 11]. It has been pointed out that either

strengthening the grid infrastructure or provision of ancillary services can be used for a secure and reliable network operation [7]. CAISO has been working in coherence with FERC to design market improvements to deal with the high unpredictable prices and disjointed price-cost scenarios [12].

Advanced metering infrastructure and a secure communication layer, being the core component of a Smart Grid infrastructure, can form the backbone for implementation of ancillary services. The problems of the ever-increasing electricity demand, aging power infrastructure, and degrading environmental impacts can be solved to an extent using the smart grid. The new vision of power management systems can be combined with two-way communication technology to create a truly intelligent system. [13].

The intermittent nature of renewable energy resources poses a challenge to their integration with the grid. Thus, power quality and reliability become important factors to consider. Bevrani, et al. [14] have surveyed the challenges and impact of DER on frequency regulation. They point out the need for new grid standards and development of mathematical models for predicting the system behavior in the presence of high penetration intermittent energy resources. The stochastic nature of renewable energy sources has also been investigated. Faria, et.al [15, 16], have used an ANN-based approach for forecasting the ancillary services. This methodology helps in predicting spinning reserves, non-spinning reserves, up-regulation and down-regulation requirements.

Better voltage and frequency regulation can be achieved using enhanced power electronics that would eventually benefit both the grid and the DG owner. On the one hand, a well designed power electronic system can be used for voltage and frequency conditioning, thus benefiting the grid; while on the other hand, the DG system could be made to coordinate dynamically to operational circumstances [6]. The benefits of inverter-based DG have been discussed in terms of regulation, reactive power compensation and power factor correction in [17, 18]. Martin Braun [7] discussed the capabilities of DG units in providing ancillary services. Each DG unit uses a different technology for grid integration. Table 2.2 sheds light on the controllability of the different coupling technologies providing grid support.

The studies undertaken by Xu, et al. [18] have shown the fast dynamic-response capability of power electronic converters to provide prompt, real-time voltage regulation.

The Renewable Portfolio Standard (RPS) mandates the states to generate a percentage varying from 4 to 30 of their total electricity using renewable energy resources [10, 19]. Such statutory laws have accelerated the renewable energy penetration in the electricity market.

There has been an economic boost in PV technology due to the ease in installation and operation, low carbon footprint and maintenance, and matching of load peaks with PV generation profiles [20]. It has also been pointed out by Raugei and Frankl [21] that a twofold increase in PV production would prune the prices by one-fifth. In [22], Liu and Bebic have correlated the extent to which voltage regulation equipment on a line can be replaced with the increase in PV inverter penetration. Even though a penetration of 5%

Table 2.2 Capabilities of grid coupling technologies [7]

Control Capabilities	IG	DFIG	SG	Inverter
Reactive Power Control	No	+	++	++
Direct Voltage Control	No	+	++	++
Improvement of Voltage Quality	No	+	No	++
Fault-Ride-Through Capability	--	+	-	++

++ Very good capability + Good capability

- Little capability -- Very little capability

No - Not possible without external equipment

IG – Induction Generator SG – Synchronous Generator

DFIG – Doubly Fed Induction Generator

has no significant effect during peak loads, a 30%-50% penetration can entirely displace the voltage regulating capacitors.

The NREL report on solar photovoltaic financing by Coughlin and Cory [23] gives data about some community PV deployments. The high installation and maintenance costs and ownership of a house with inadequate sunshine are a few reasons that make community based PV systems rank above roof-top PV systems, along with the economic benefits related to power integration with the grid. The Ellensburg project, Sacramento Municipal Utility District (SMUD) SolarShares Program and the SunSmart Community Solar project in St. George, Utah are few examples of the community based PV installations. The economies of scale based on decoupled yet aggregated PV systems on an energy and system basis has also been discussed. The Ellensberg system had an installation of 57 kW in 2008 with 24-30 kW increase in 2009. SMUD launched a 1 MW solar farm in concurrence with the SolarShares program. Further, the St. George Services Department set up a 100 kW community PV system in collaboration with the regional cooperative electric company, Dixie Escalante in 2008. The report also discusses lucrative initiatives like the Solarcity's Community Solar Discount Program in San Jose and the Mosier Creek Project in Oregon.

The Electricity Advisory Committee report [24] describes the current state of the energy storage devices as a key component of the futuristic smart grid with renewable generation. Researchers are working on energy storage systems for a very long time to make power systems more reliable as well as to make renewable energy sources more dispatchable. Reference [25] states that, provision of spinning reserves, load leveling and forecasting, frequency and voltage regulation, reactive power support, improved power quality and reliability of the system and efficient management of capital are the benefits provided by them depending on the technology employed. Vartanian [26], describes the

use of A123System deployed, 20 MW Nanophosphate Li-ion battery-based systems providing ancillary services in different state of US and California, since 2008. The author outlines the usage of the storage units for frequency regulation as a result of higher wind penetration and also improvement in the recovery of a system after a failure. Battery technology has been found promising due to its modular nature, environment friendliness, quiet operation and swift installation at almost any location [27].

Tapanlis and Wollny [28] have proposed voltage and frequency control of microgrids and minigrids with PV, wind and battery through AC coupling. Borlea, et al [29] have proposed an optimal solution for the provision of ancillary services at the substation level. They have considered the use of a fuel cell plant as a backup resource for system support in this study.

A micro-grid with PV-based active generation has been analyzed for its capacity to provide ancillary services by Lu and Francois in [30]. There is a signal being exchanged between the central power management of the grid and local power management of the generator. A droop controller has been used to solve the problem of real time power management and planning, based on load and power forecasting for individual sources and loads.

Liu, Zhou and Li [31] proposed a power management scheme with successive multilevel inverters integrated to the grid to control active and reactive power from PV and an energy storage system. An active and reactive power management (ARPM) strategy based on dual stage discrete Fourier transform [DFT] phase locked loop [PLL] was employed for reactive power management between PV and batteries.

Sun et al. [32] have interfaced the PV generation system and battery with the grid using DC/DC converters for the PV arrays, DC/AC Converters for grid connection and DC/DC converter for a battery. The DC-bus signals prompt the switching between constant voltage and MPPT operations. Four modes of operation, including islanding have been studied. The authors have further eliminated the battery faults due to over-or-under charging.

Tina and Pappalardo [33] have described a power management scheme at the end-user level, with a PV and a battery storage system. They have achieved multi-mode operation of the system by coupling the individual sources on the AC side using inverters.

The above literature review clearly lays down the foundation of this research in terms of the importance of PV in the present power market that is eventually taking a leap towards the Smart Grid. It further motivates one to find solutions to the open issues with regards to the integration of these valuable resources at high penetration levels with the future grid.

3. P-Q CAPABILITY

3.1 PROPOSED POWER MANAGEMENT SCHEME

Fig. 3.1 shows the proposed scheme for providing frequency and voltage support to the grid that increases grid friendliness. A two-way communication between the grid and the distributed energy resource (DER) is assumed. By having such an important link, they can exchange information and keep the system updated about the current health. The PV system with the energy storage discussed in this thesis is only a part of the entire regulation idea. Many such dispersed sources can form their own resources and can participate in regulation. Contribution of the active and reactive power from the multiple resources can bring significant changes in system parameters such as frequency and voltage. The idea proposed here is to generate the capability limits of the individual system and transfer them to the operator. The operator receives the active and reactive power capability limits at specific time intervals from the individual DERs and can synthesize it according to the utility's need. Each DER will send its capabilities every 5 to 15 minutes so that the operator will have the most updated status report. Since updates of the source occur frequently, the reliability of the source providing the regulation can be assured. During the regulation period, the operator sends the command signals to each DER demanding active or reactive power for specific amount of time resulting in the frequency and voltage change towards the nominal values of the system.

3.2 ACTIVE AND REACTIVE POWER CAPABILITY

The P-Q capability is the ability of the system to provide active and reactive power instantaneously. An intelligent controller implemented here is responsible for

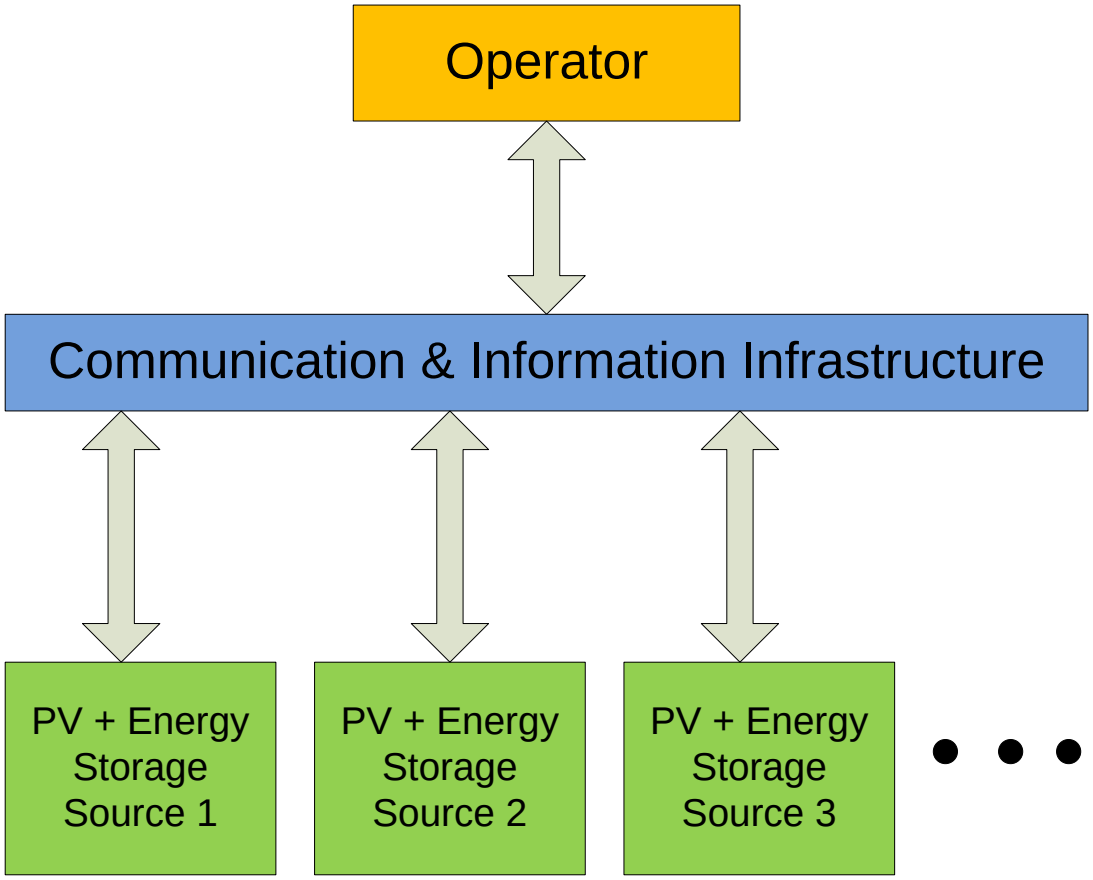

Figure 3.1 Proposed scheme for frequency and voltage support

generating/absorbing the maximum active power (±P) and generating/absorbing the maximum reactive power (±Q) that the system can handle. It measures the power output of the PV system and the state of charge (SOC) of the battery and decides how much energy can bedelivered/absorbed at a given moment. The nominal voltage of the battery is 240 volts and its capacity is 11 Ah. Assuming that the state of charge of the battery is 50%., the amount of energy that can be absorbed or released from the battery is 240x5.5Ah = 1.32 kWh; depending on the charge/discharge rate, its capability can be defined as 15.84 kW for 5 minutes, or 7.92 kW for 10 minutes or 5.28 kW for 15 minutes. Currently, standards such as IEEE 1547 and UL1741 state that the PV inverter

cannot participate in regulating voltage at the PCC [34]. Therefore, PV inverters are forced to operate at unity power factor. However inverters are capable of providing reactive power along with the active power. One major advantage of having an inverter in the system is that its reactive power can be varied continuously. The apparent power rating (S) of the inverter can be resolved into components of P and Q given by Eqn. 3.1:

$$S = \sqrt{P^2 + Q^2} \qquad (3.1)$$

Depending on the inverter rating and the amount of DC power available at the input, the P-Q capability of the inverter can be determined as shown in Fig. 3.2.

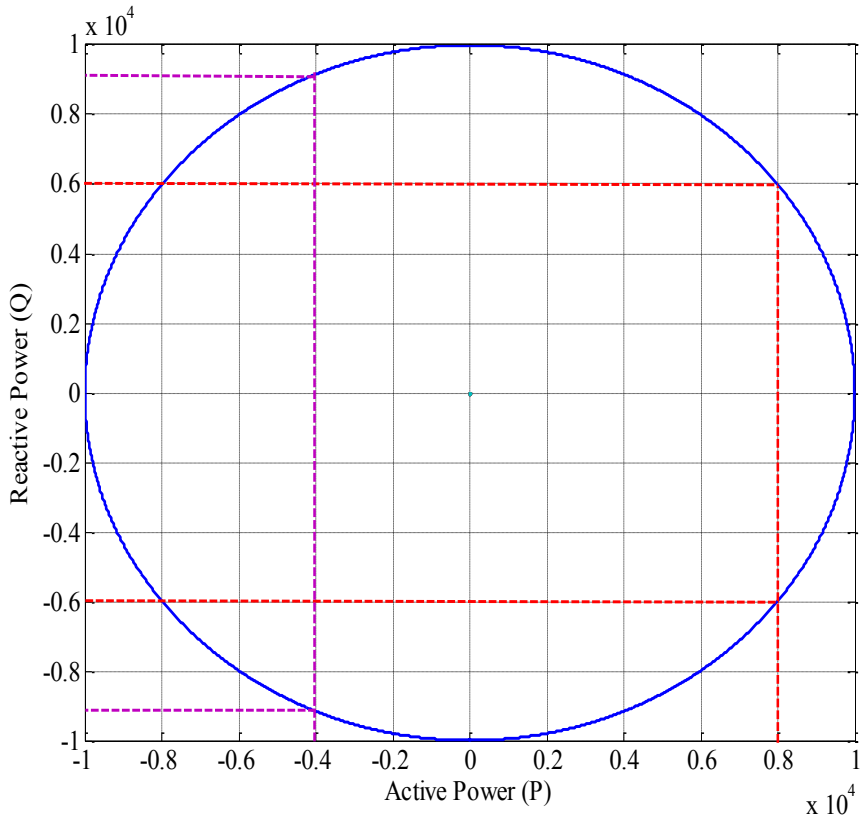

Figure 3.2 The P-Q capability of a 10 kVA PV inverter

The circle plotted in Fig. 3.2 is the boundary of the 10 kVA inverter. By means of proper switching, the inverter can be operated in a four-quadrant mode. One can see from Fig. 3.2 that if 8 kW is the amount of DC power available at the input, then by introducing the proper phase to the output current, the inverter can deliver 6 kVar of leading or lagging reactive power. Similarly for P_{in} = - 4 kW i.e. when bridge is operating as active rectifier, it can deliver/absorb 9.16 kVars. If the power at the dc bus (P_{dc}) is equal to S, then the inverter loses its reactive power capability; on the other hand, if P_{dc} is zero, then the inverter capacity can be dedicated to provide reactive power only. However, there are some losses associated with the inverter, and so, P_{dc} cannot be zero. The proper inverter size can be selected in order to provide a specific amount of voltage regulation. The normal practice is to select an inverter with $S = P_{dcmax}$ where P_{dcmax} is the maximum active power that the inverter injects into the grid. Over-sizing the inverter just by 5% provide 32% additional capacity of reactive power as shown in the power triangle of Fig. 3.3.

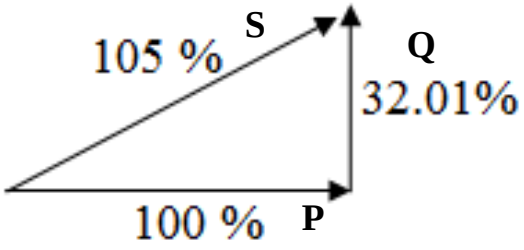

Figure 3.3 Effect of inverter size on the reactive power capability

3.3 GENERATING CAPABILITY

The command signal demanding regulation lasts for a few minutes. Depending on the amount of power required, it can last from 5 to 15 minutes. Therefore, the energy density of the system must be known. The battery modeled in this thesis has a nominal energy density of 2.64 kWh. If the state of charge of the battery is known, then by using Eqns. 3.2 and 3.3, an active power capability curve of the system can be plotted. Since the apparent rating of the inverter is known, the reactive power capability is easy to find.

$$E_{available} = \frac{SOC(\%)}{100} \times 2.64 \text{ kWh} \tag{3.2}$$

$$E_{available} = P \times t \tag{3.3}$$

3.3.1 Up regulation Capability: Fig. 3.4 shows the system's up regulation active power capability. Different curves for three different SOC are plotted using Eqn. 3.2 and Eqn. 3.3. These curves are only a function of the battery SOC while the PV array has zero contribution. When there is any frequency or voltage variation on the grid side, the PV power is also accountable for it. Since the proposed system is a community-based PV system, it is assumed that the amount of power the PV array produces is injected directly into the grid. The capability curves thus generated are sent to the utility operator. Based on the current battery SOC, only one curve will be available to the operator. For example, if the battery SOC is 50%, then only the middle curve of Fig. 3.4 would be available. One can see from the curve that if the amount of active power demanded is 10 kW, then the system can supply 10 kW for 8 minutes only. An active power of 10 kW for 8 minutes accounts for 1.32 kWh of energy which is 50% of the nominal battery capacity. After 8

minutes, the battery would be completely depleted. Regulation signals are time based signals, i.e., there is a demand of active power for specific amounts of time varying from 5 to 15 minutes. For 50% SOC, the product of demanded active power and the time should not exceed 1.32 kWh .One can see that for 50% SOC, the battery can provide 15.8 kW for 5 minutes; however, the inverter imposes a limitation on this capability. The maximum active power that the inverter can handle is 10 kW (since the inverter is sized at 10 kVA) and draws a boundary around the capability curve. The area under the curve and below 10 kW is the system's ability to provide frequency regulation. The data thus generated is sent to the operator and is updated every 15 minutes.

3.3.2 Down Regulation Capability: Down regulation capability is a function of the energy coming from both the PV and the battery. The presence of the PV increases the down regulation capability. Consider a case where the PV array is producing 1500 watts at 800 w/m^2. For the next 15 minutes, the energy available from the PV array can be calculated as 1500 watts x 0.25 Hours = 375 Wh.

$$E_{available} = E_{batt} + E_{pv} \quad (3.4)$$

$$E_{available} = 1.32 \text{ kWh} + 0.375 \text{ kWh} = 1.695 \text{ kWh}. \quad (3.5)$$

Based on Eqn. 3.4 and 3.5, the down regulation capability can be plotted for different battery SOC and is shown in Fig. 3.5. An SOC of 70% indicates the current state of the charge of the battery and the battery can be charged further for the remaining 30%. One can see that the capability of the battery to charge is higher in the case of 20% SOC than 70% SOC.

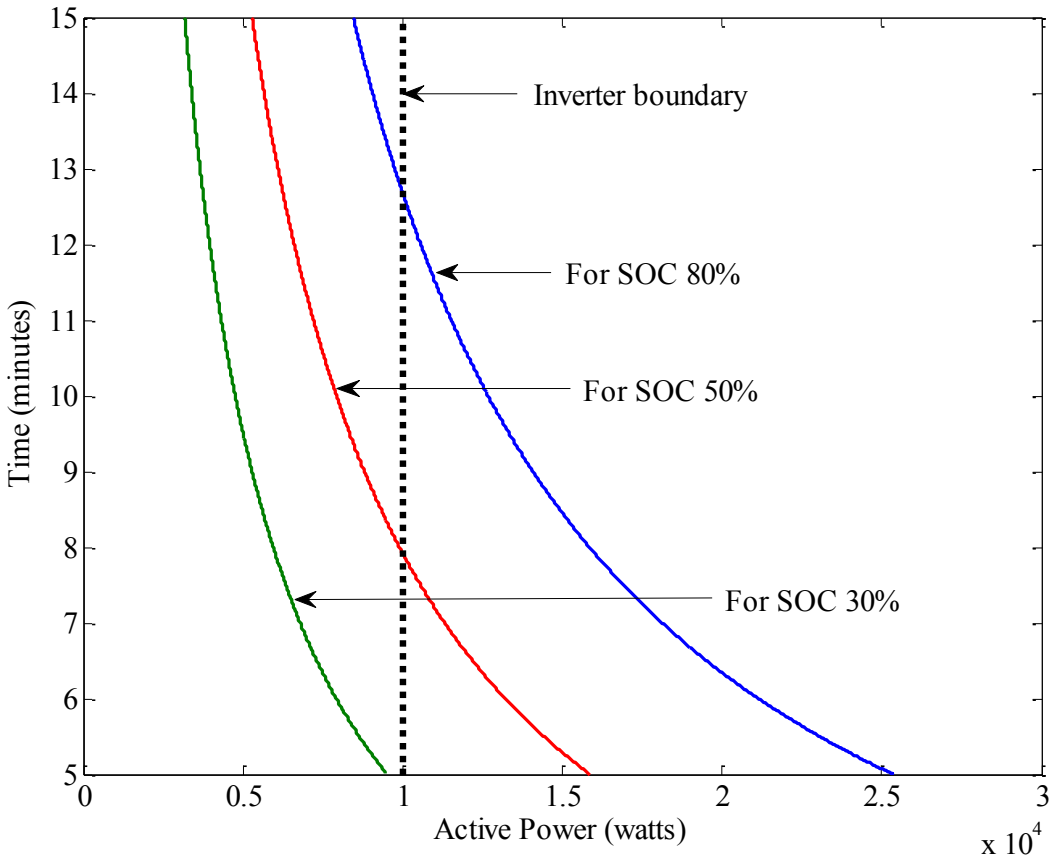

Figure 3.4 Up regulation capability for variable SOC

The envelope shown by dotted lines above and below each curves shows the effect of variations in the insolation. Since the system updates its health every 15 minutes, there is a likelihood that the solar insolation will vary somewhat during this interval. As shown in Fig. 3.5, the upper and lower boundary around the main curves indicates a ±20% change in insolation. The system's capability to absorb energy can be further increased by tracking the pseudo power point on the PV curve [35]. The method discussed in [35] shows that active power injected from the PV can be effectively

controlled from the maximum power to almost zero. This results in increased flexibility when the battery is not available.

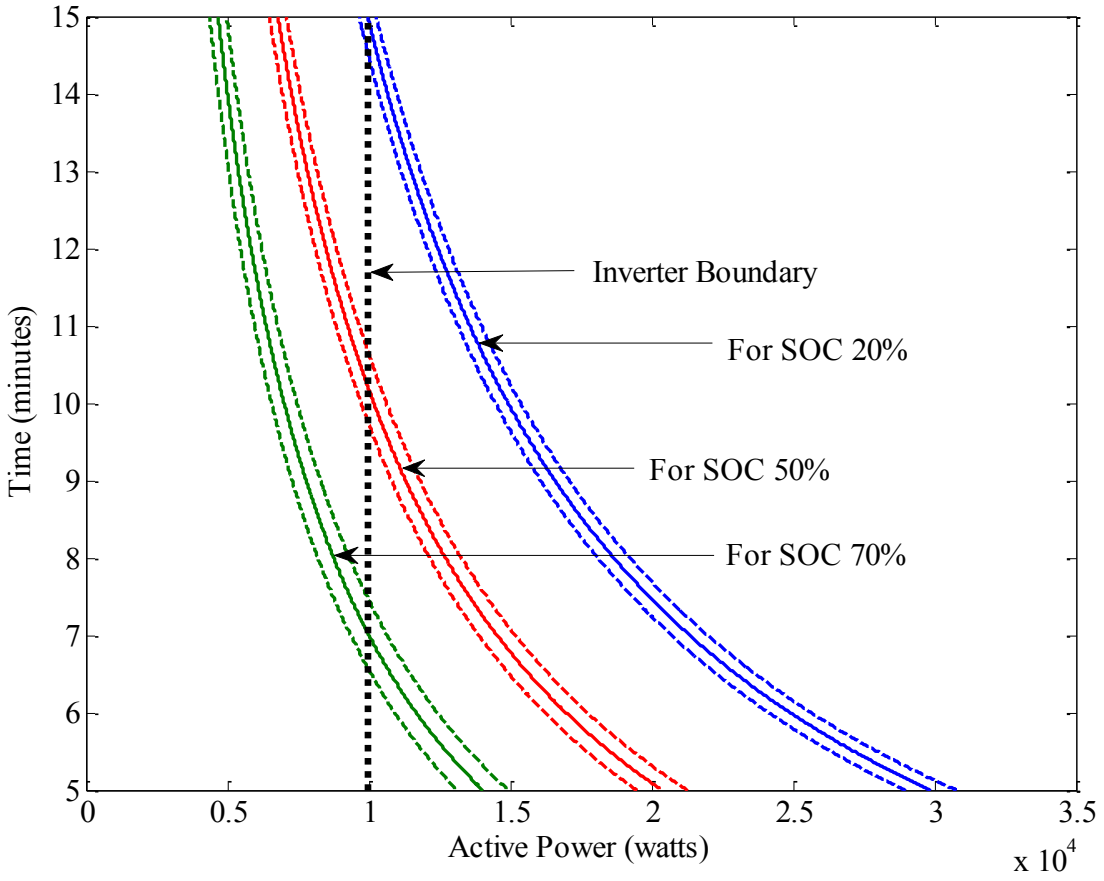

Figure 3.5 Down regulation capability curve for variable SOC and Ppv = 1500 W

Batteries are the storage devices which cannot be overcharged or depleted completely. Their charging/discharging has to be controlled in order to maintain it for longer life. This care can be taken while generating the capability. Let's assume that

battery is at 80% SOC and the requirement is that battery should not be discharged below 20%. In this case, one can generate the capability curve for only 60% SOC. Thus, the battery is contributing only up to 60%, and the rest 20% of the charge is always in reserve. Similarly, the up regulation capability curves can be generated where batteries are not allowed to charge above 90% of its capacity.

Along with the up and down regulation capabilities, the inverter's rating S is also available to the operator. By referring to Fig. 3.2, Eqn. 3.1 and the active power demand, the reactive power capability of the system can be identified. The operator generates command signals for both P and Q to send to the system through a dedicated communication channel. The system controller acknowledges the command and provides appropriate switching in order to fulfill the demanded quantities. This is addressed in detail in Sections 4 and 5.

4. SYSTEM DESCRIPTION

4.1 BLOCK DIAGRAM

A block diagram of the system model is shown in Fig. 4.1. The system is implemented in two-stages of power conversion: dc-dc and dc-ac. It has three independent control loops for the dc-dc converters and the three-phase dc-ac inverter. The system comprises of:

- PV panels with MPPT tracking
- Batteries with controlled bi-directional dc-dc converter
- Three phase inverter with delta modulation scheme

For the system shown in Fig. 4.1, a boost converter is used to track the maximum power from PV panels; a bi-directional dc-dc converter connects batteries to the dc link and provides power required for regulation, and an inverter, controlled by delta modulation, controls the dc link voltage and injects power into the grid at a desired power factor. This topology can provide almost instantaneous power transfer capability.

4.2 PV ARRAY

As shown in Fig. 4.2, a single diode model of the PV cell is used to simulate PV characteristics in Matlab Simulink [36]. The effect of temperature on panel voltage is taken care of in the model.

The governing equation of the model is given by (4.1)

$$I_{pv} = I_{ph} - I_o\left(e^{\left(\frac{V_{pv}+I_{pv}.R_s}{A.V_t}\right)} - 1\right) - \frac{V_{pv}+I_{pv}.R_s}{R_p} \qquad (4.1)$$

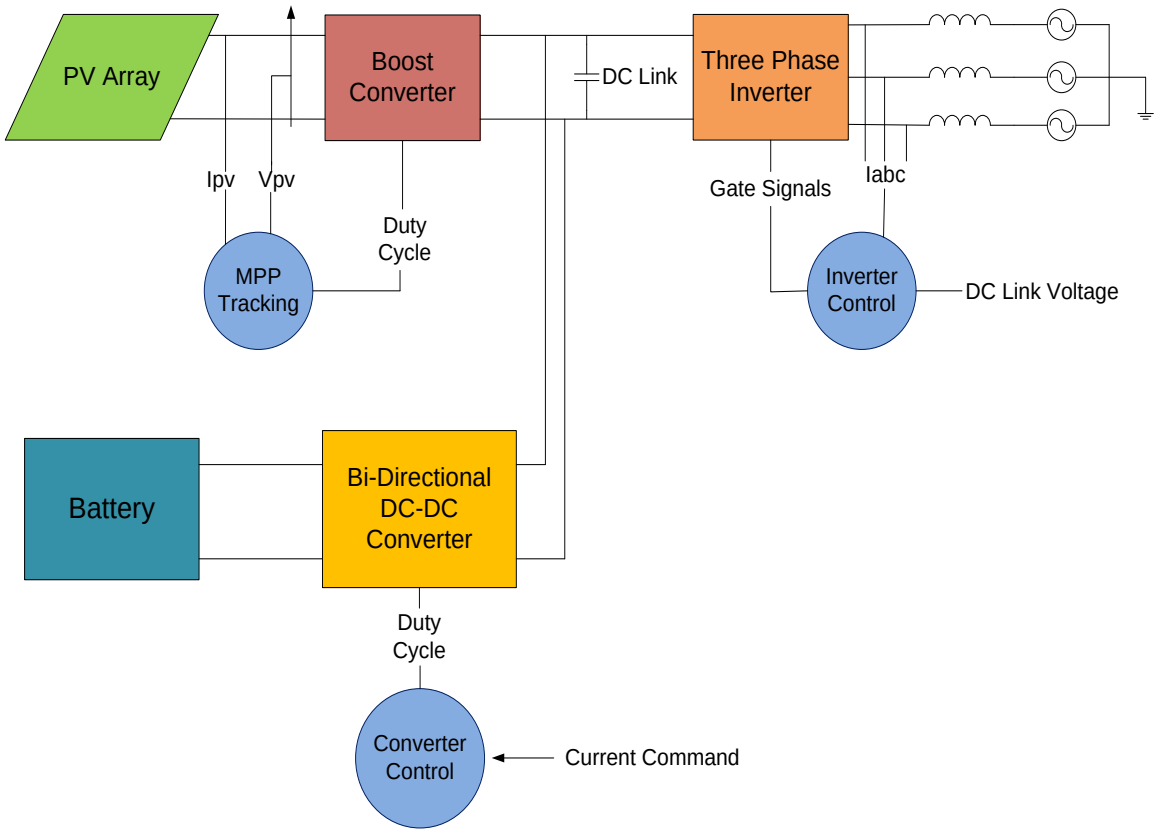

Figure 4.1 Grid connected PV system with energy storage

Where,

I_{pv} - Actual PV current

I_{ph} - Photocurrent

I_0 – Saturation current of the diode

V_{pv} - PV cell voltage

A – diode quality factor = 1.4

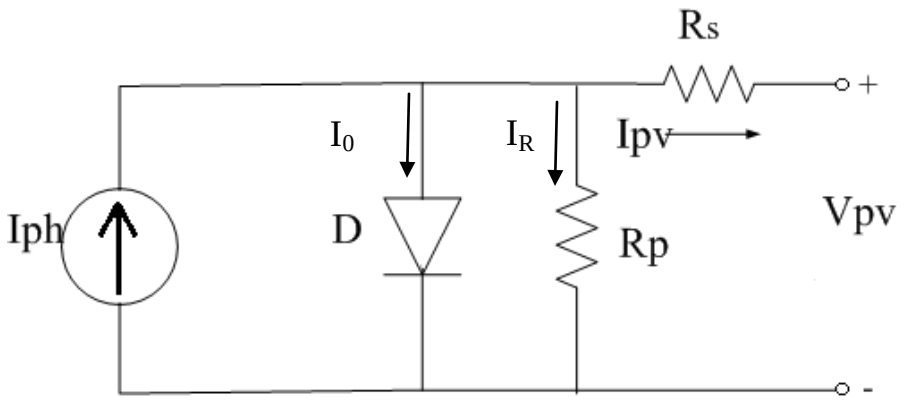

Figure 4.2 Single diode model of PV cell

R_p – Equivalent parallel resistance

R_s – Equivalent series resistance

The PV cell current I_{pv} is composed of three current components: I_{ph} is a direct function of irradiance and temperature, I_0 is the diode current exhibits cell's p-n junction characteristics and third component is I_R flowing through the equivalent parallel resistance. Panels are placed in series to increase the voltage and they are placed in parallel to increase the current. A combination of both increases the net power of the PV array. A GE-PV 200W solar panel is used to build a 2 kW PV array [37]. The PV panel's datasheet parameters are given in Appendix A. To build a 2 kW array, five panels are connected in series in order to reach the desired voltage (26.3*5=131.5 V), and two such strings are connected in parallel to deliver the desired amount of current (7.6*2 = 15.2 A).

The open source PV model developed by University of Colorado Boulder is used as a reference to build this array in MATLAb/Simulink [38]. Model's accuracy can be found by comparing simulation results to the real world values. Fig. 4.3 shows the typical I-V characteristics given by the manufacturer and Fig. 4.4 shows the characteristics obtained from MATLAB simulation. The curves are almost the same.

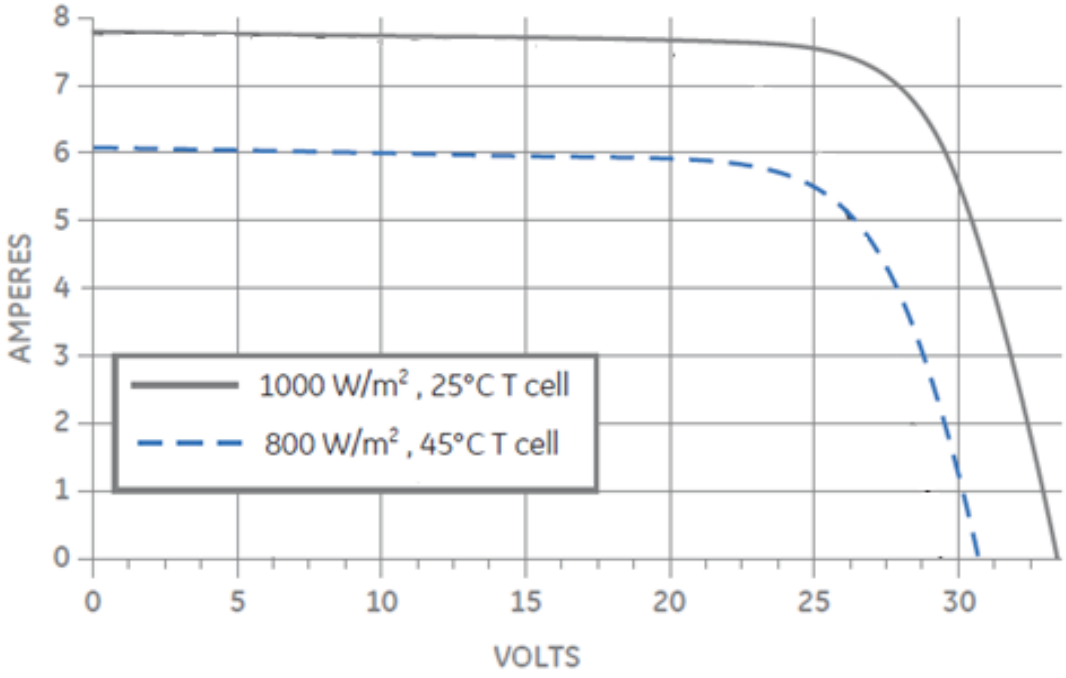

Figure 4.3 Typical I-V characteristics of GE-PV 200 W panel

4.3 MPPT CONTROLLER

The P-V characteristic of the PV panel is non linear in nature. Due to the moment

to moment variation of insolation, temperature and cell characteristics, there is a need to track the maximum power from the PV array.

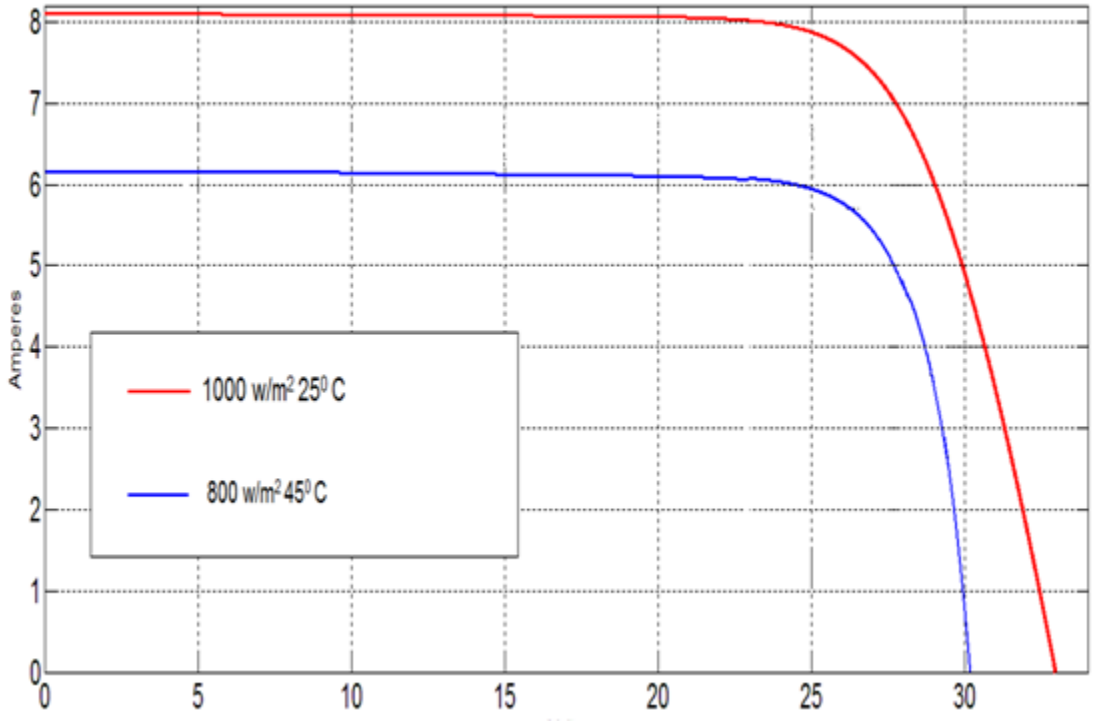

Figure 4.4 I-V curves from the MATLAB model

The *dp/dv* method [39], shown in Fig. 4.5 is used to track the maximum power output. The method is simple and independent of panel parameters. The operating current and voltage of the array are constantly monitored and the difference in these variables is checked at every instant of time. The difference between the current and the previous values of power is checked to determine the sign of the slope on the power characteristic

curve. The slope thus calculated is used to generate the reference voltage. A PI controller uses this reference voltage to generate the switching pulses for the boost converter shown in Fig.4.6. A new reference value indicates that the operating point is moving towards the MPP. This process is repeated until the slope of the P-V characteristic is zero, i.e., the MPP has been tracked.

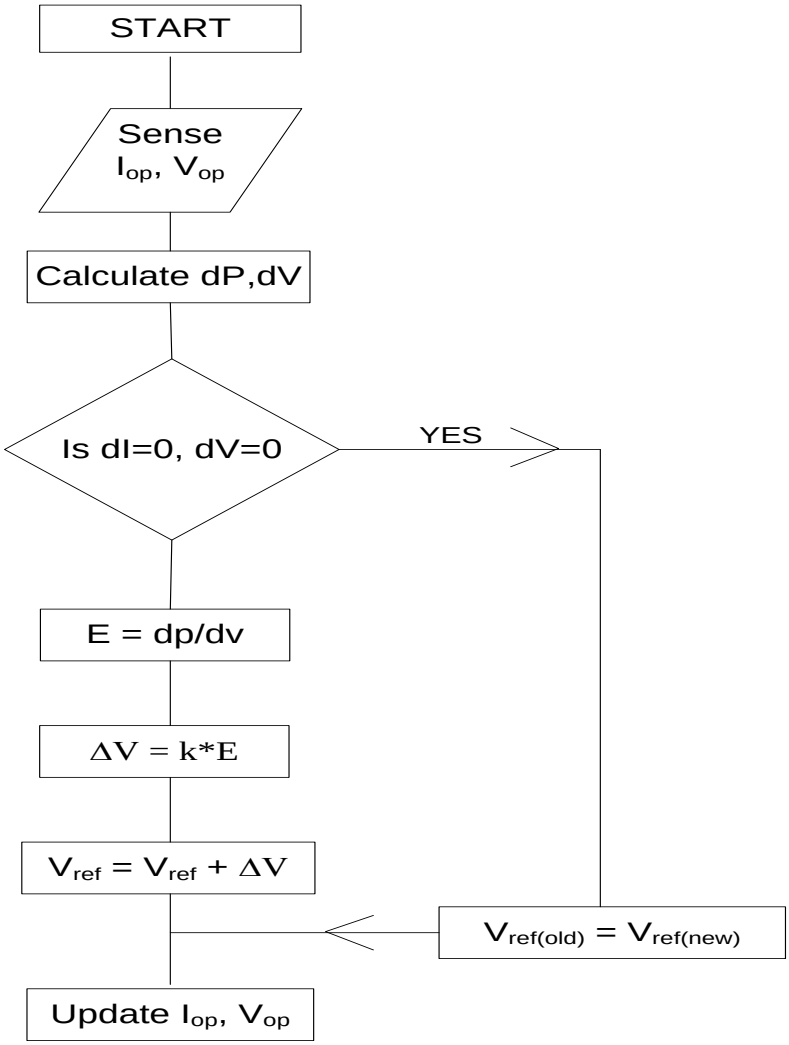

Figure 4.5 MPPT algorithm – the *dp/dv* method

As shown in Fig. 4.6, the boost converter is responsible for tracking maximum power available at the PV array. It delivers energy at the dc bus by boosting the voltage to 400 Volts. The MPPT works effectively if the DC bus voltage remains constant; thus a

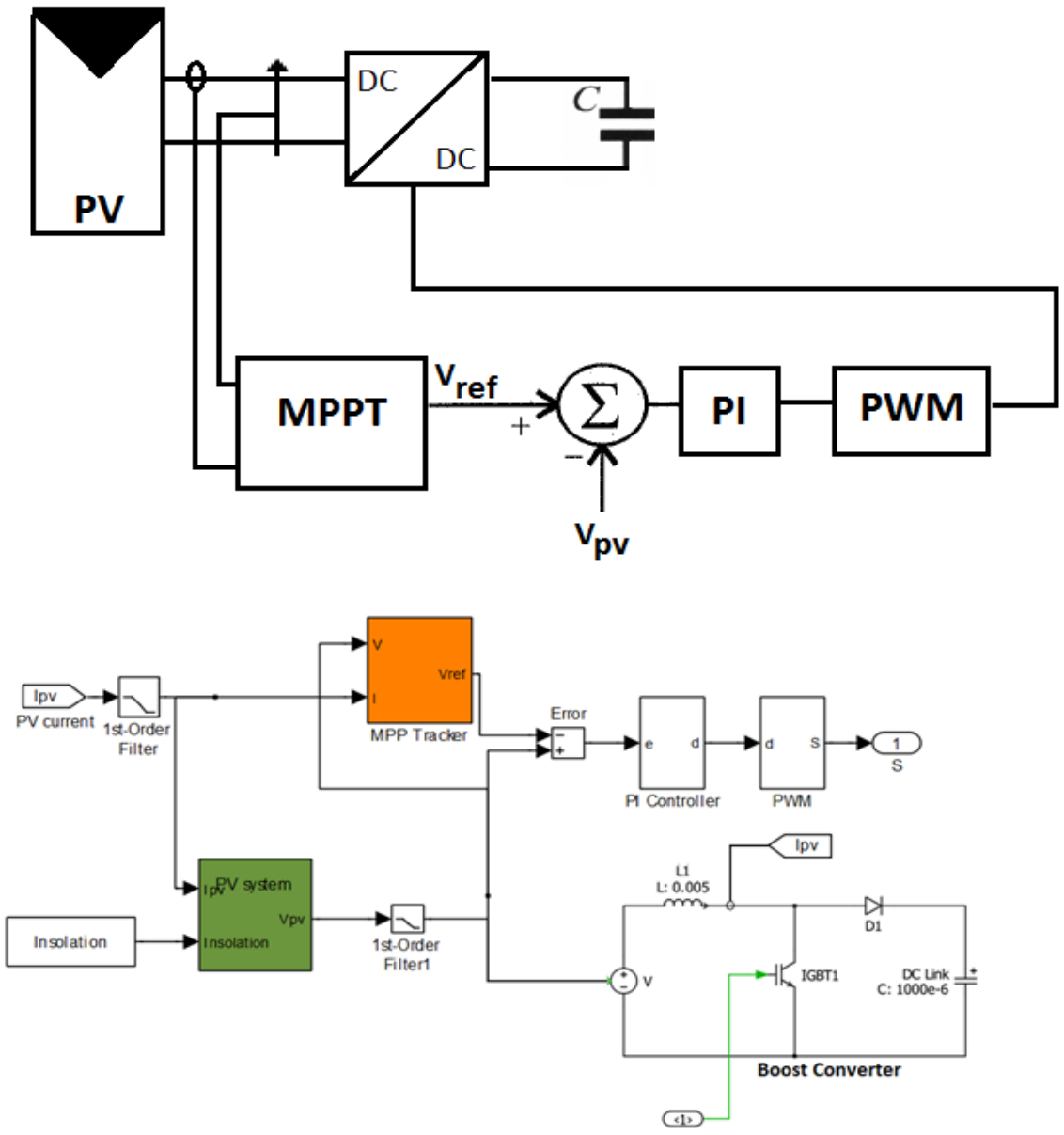

Figure 4.6 PV with maximum power point tracking implemented in PLECS

second controller is designed for regulating the DC link voltage. The second controller is discussed later in this chapter.

For the boost converter,

$$V_{in} = L\left(\frac{\Delta I}{DT}\right) \tag{4.2}$$

Where $T = 1/f_{sw}$ (switching frequency is selected to be 20 kHz)

$$D = 1 - \left(\frac{V_{in}}{V_{out}}\right) \tag{4.3}$$

$$D = 1 - \left(\frac{131.5}{400}\right) = 0.671 \tag{4.4}$$

Under maximum insolation, the array can deliver 2 kW of power. For 2 kW of power and input voltage of 131.5 volts, maximum current is 15.209 Amps. The lesser the current ripple, the larger would the size of the inductor have to be. A usual design practice is to have 10 % current ripple but in this case 6% current ripple is chosen. The current of the boost converter is fed back for tracking purpose. Less oscillation in the current results in reduced oscillation around the maximum power point. From Eqn. (4.2), (4.4) and the assumed designed parameters, the inductor chosen to be 5 mH.

4.4 BATTERY

In the proposed system, batteries are used to help in decreasing the adverse impact of intermittency of the PV source. Batteries possess a high energy density and provide power at almost constant voltage if the charging/discharging cycles can be properly

controlled. Fig. 4.7 shows the simple battery model implemented in Matlab. It is a controlled voltage source in series with a resistance whose control input E is a function of the state of charge. If a discharge curve of the battery cell is known which is generally given by the manufacturer, then finding the parameters such as A, B, K and E0 is simple and given in [40].

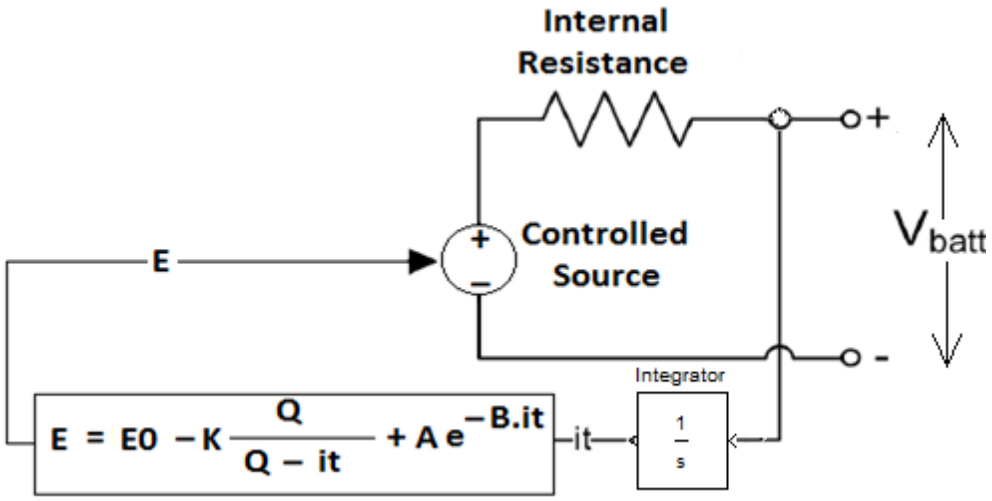

Figure 4.7 Battery model [40]

Table 4.1 shows the parameters of a single Li-ion cell and taken from [40]. These parameters are used to build a battery with the capacity of 11 Ah and a nominal voltage of 240V. 67 cells are connected in series and 11 cells in parallel in order to build a battery pack. Fig. 4.8 shows the discharge curve and it can be seen that after the exponential zone battery voltage is nearly constant. The battery is discharged at 1C rate i.e. at 11A. Based on the voltage profile, the battery is operated between 20% to 80% SOC throughout the

simulations, so that the battery terminal voltage can be assumed to be constant at 240 volts.

Table 4.1 Li-ion battery parameters

Parameters	Lithium-ion Cell 3.6V, 1 Ah
E0 (V)	3.7348
R (Ω)	0.09
K (V)	0.00876
A (V)	0.468
B $(Ah)^{-1}$	3.5294

4.5 BI-DIRECTIONAL DC-DC CONVERTER

The battery thus modeled is integrated in parallel with the DC link via the bi-directional dc-dc converter as shown in Fig. 4.9. This converter is responsible for charging or discharging the battery. Therefore, when the battery is injecting power into the grid, the converter will operate in the boost mode, and, when the battery is absorbing power from the grid or the PV panels, the converter will operate in the buck mode. The system follows Eqn. (4.5) to manage power flows on the dc side.

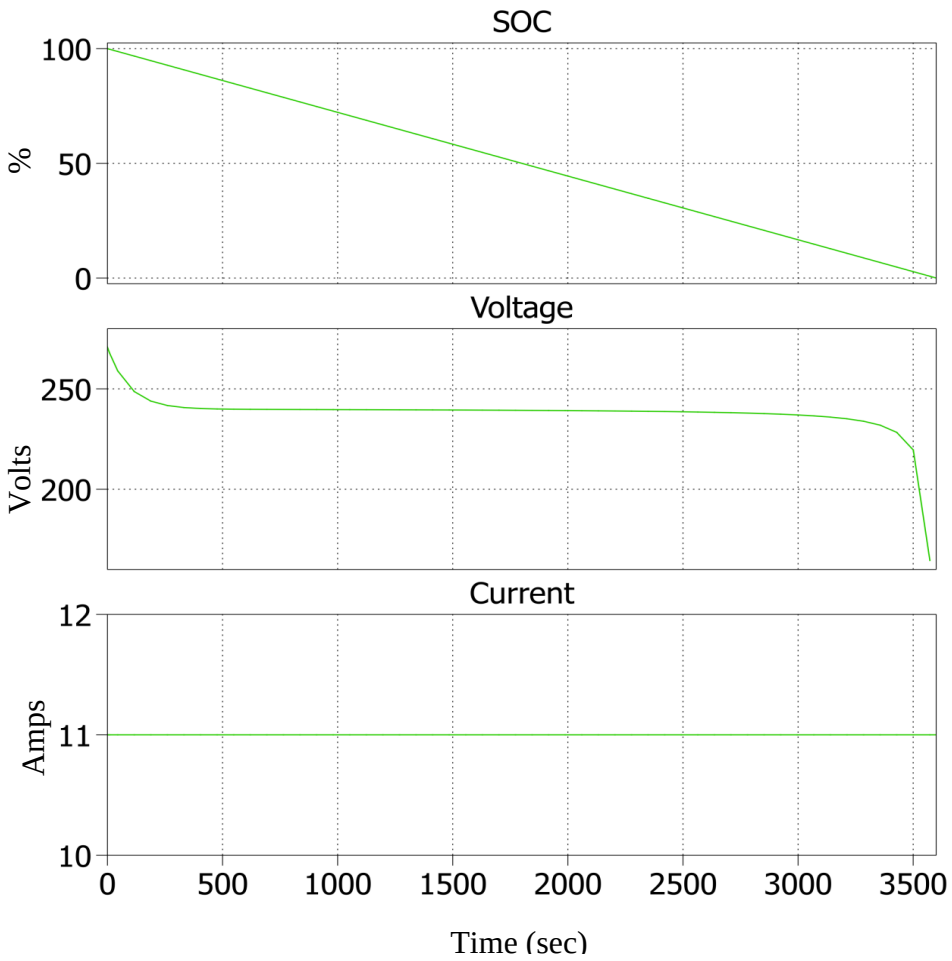

Figure 4.8 Discharge curve of a 240V, 11 Ah Li-ion battery

$$\mathbf{P_{batt}} = \boldsymbol{P}_{\mathbf{grid}} - \boldsymbol{P}_{\mathbf{PV}} \qquad (4.5)$$

As shown in Fig. 4.9, the reference current is generated from the power commanded by the grid operator. This reference current is compared with the inductor current and the error thus produced is maintained within bands. The control strategy is similar to hysteresis current mode control [41]. Hysteresis control is very effective and it is simple to implement.

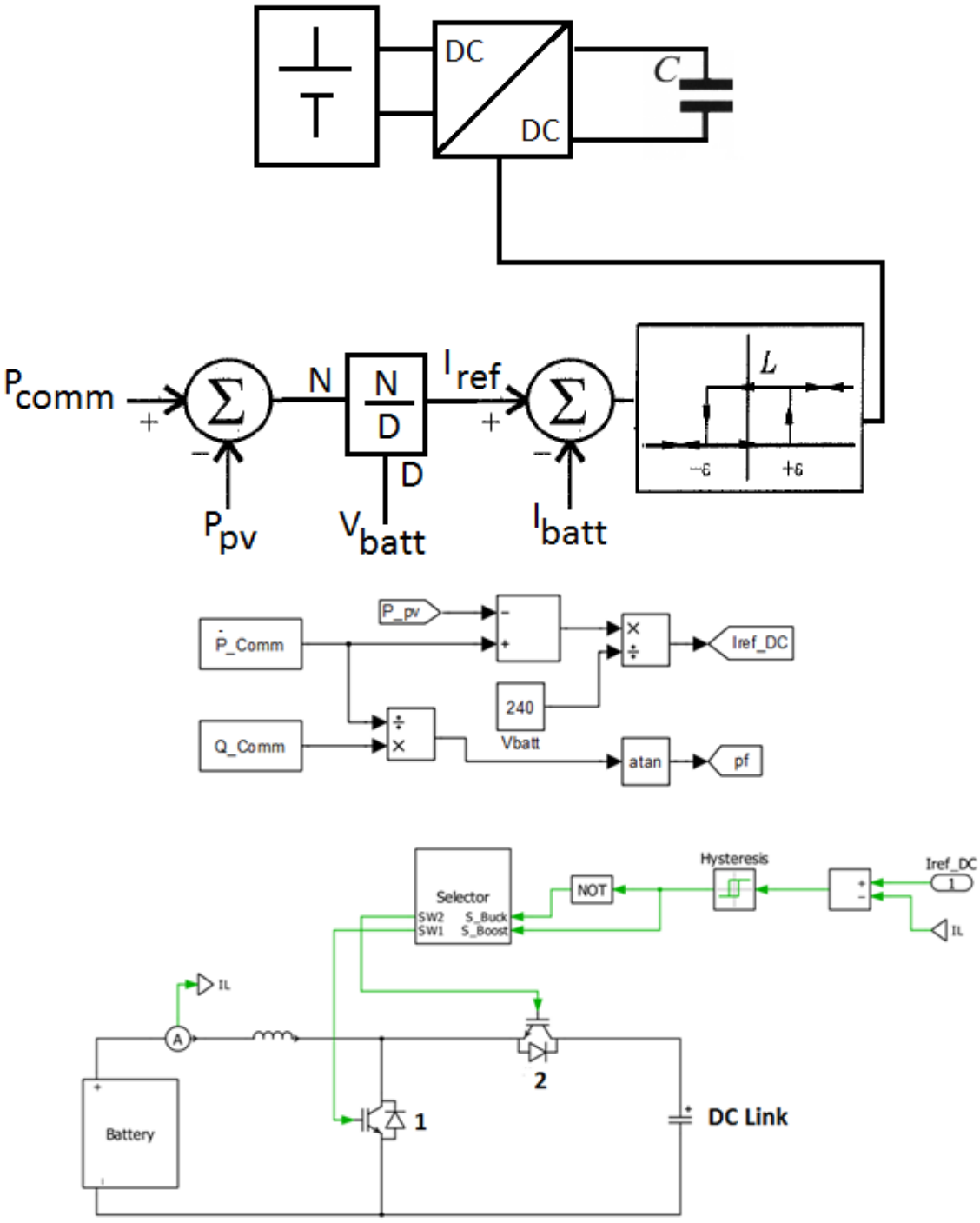

Figure 4.9 The bi-directional DC-DC converter with control implemented in PLECS

One very common drawback of hysteresis control is that the switching frequency is not constant. Fig. 4.10 shows the hysteresis band set for the converter. If the converter is operating in the boost mode, switching pulses are given to switch 1, while switch 2 operates as a diode. On the other hand, if the converter is operating in the buck mode, switching pulses are given to switch 2, while switch 1 works as a diode. The commanded current Iref_DC is the average value of the DC current required to have the desired power transfer. The inductor current is compared to Iref_DC and if the error touches the upper boundary, no switching pulses are given to the switch. This allows the inductor to discharge and thereby, the current flowing through inductor, falls. As soon as the inductor current intersects the lower boundary, switching pulses are provided to IGBTs 1 or 2 depending on the converter's mode of operation. This control strategy is independent of the direction of the power flow and generates switching signals for both the buck and the boost modes. An intelligent controller selects the mode of operation based on the sign of the P_{batt} and passes the pulses to a designated semiconductor switch. The decision on whether the converter operates in the buck or the boost mode is based on the command signal received from the grid. If a regulation signal is not received, and the battery needs to be charged, then the battery SOC is the variable used in deciding whether the converter needs to be operated in the buck mode. If a regulation signal is not received, the battery is disconnected from the rest of the system.

Thus battery current will always have 3A peak to peak ripple with the average value correspond to the commanded dc power from the battery. From Eqn. (4.2), one can say that if the input voltage of the converter is constant and the hysteresis band is set to the ripple current ΔI and for the designed inductor value, the switching frequency of the

converter is constant. In this case, the input voltage of the converter changes the switching frequency. For an input voltage of 240 V, ΔI = 3A and f_{sw} = 15 kHz, the inductor value from Eqn. (4.2) is found to be 2.133 mH.

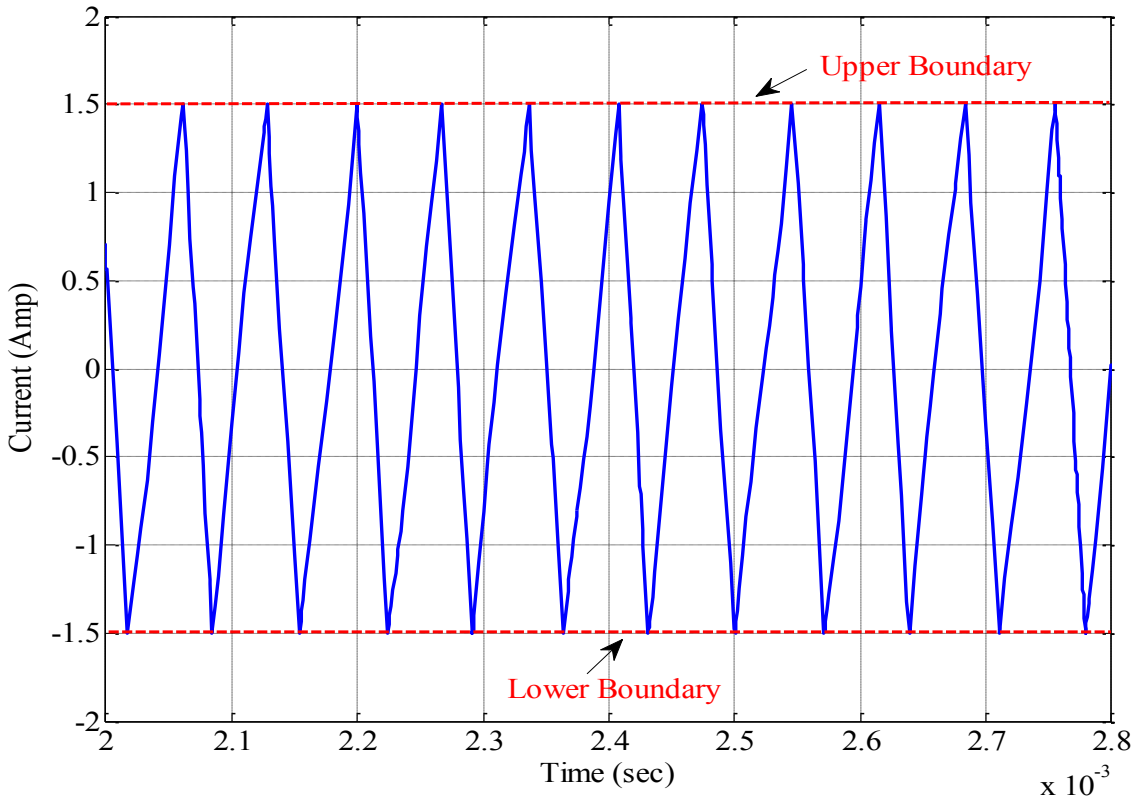

Figure 4.10 Hysteresis band for the bi-directional DC-DC converter

The DC link capacitor plays a very important role in the operation. In the boost converter, the ripple current that the output capacitor handles is the output current of the

power stage. Since the DC link capacitor is connected at the output of two boost converters, it should be able to handle the output currents of both stages. In addition, it needs to absorb or supply the ripple current associated with reactive power, and the ripple current at the switching frequency of the inverter, which is variable. The math involved to find the rms. capacitor current is complicated; therefore, the capacitor value is chosen from observing the ripple at the DC bus from simulations. In order to keep the voltage ripple below 1% of 400 volts, the capacitor value selected is 1000 μF.

4.6 INVERTER WITH DELTA MODULATION

The inverter is responsible for converting the dc power from the PV/battery system into ac for output to the grid at the desired power factor. It also acts to convert the ac power from the grid to dc for charging the batteries. The three phase bridge shown in Fig. 4.11 is controlled by the delta modulation scheme [41]. It is also responsible for regulating the voltage at the DC link.

To have the desired reference AC currents at the output, the magnitude and phase information is essential. A simple PI loop generates the magnitude of the current by comparing the DC link voltage to the reference value, and a phase locked loop provides the voltage phase angle information. Thus PI controller takes care of the voltage at the dc bus. The controller generates a positive reference current for a positive error and a negative reference current for a negative error. By introducing an additional angle θ, the power factor of the bridge can be controlled. If the voltage at the DC bus increases, that means additional energy is available at the DC bus and needs to be transferred to the grid side.

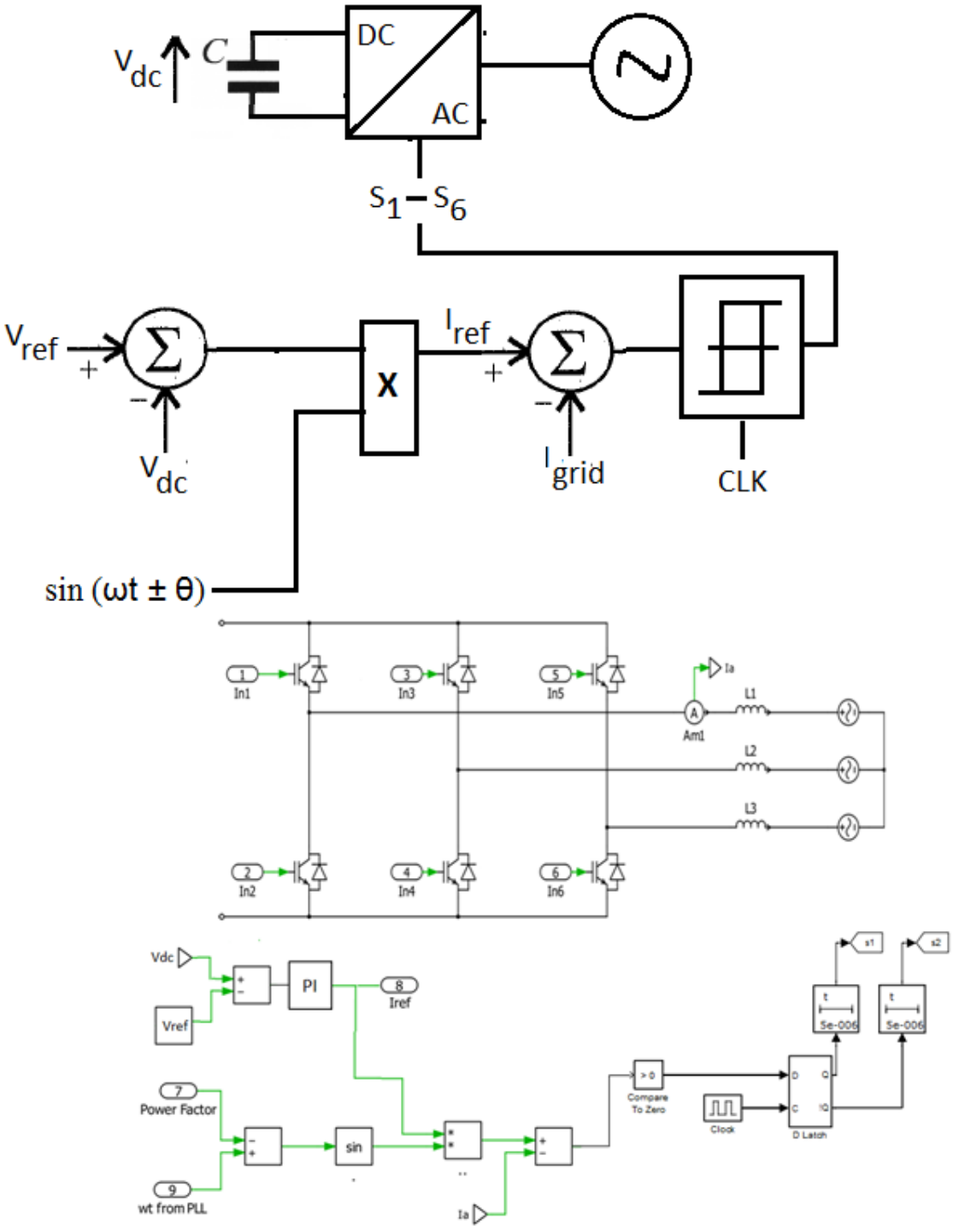

Figure 4.11 Inverter with delta modulation control of phase A implemented in PLECS

The PI controller generates a positive reference current and the bridge operates as an inverter. On the other hand, if the battery is absorbing power, then the DC link voltage drops and the controller generates a negative reference current, operating the bridge as an active rectifier. It takes energy from the grid and regulates the DC link voltage. The reference current generated is in the form of I_{ref}*sin ($\omega t \pm \theta$) and represents the total three phase power. This current is divided by 3 to generate single phase currents. The reference currents for other two phases are generated by introducing 120^0 displacement. All the reference currents are compared to the actual per phase currents. The error thus produced latches the D flip-flop and passes the pulses to the respective switches. A positive error means that the current has not reached the reference value, and so, the D flip-flop passes the clock pulses to the upper IGBT of phase A and the lower IGBT is turned OFF in order to prevent short circuit. The lower IGBT is turned ON and the upper IGBT turned OFF when a negative error resets the flip-flop.

Since sinusoidal current tracking is involved, the switching frequency of the bridge is not constant. However, the maximum switching frequency can be controlled by controlling the clock frequency. This is the advantage of delta modulation control technique over Hysteresis control [41]. In this thesis, the clock frequency is set to 20 kHz. The wave shape of the AC current is mainly dependent on the filter at the output and the switching frequency. The higher the switching frequency, the more accurate the tracking would be.

4.7 INTELLIGENT CONTROLLER

The control scheme selected for this system is simple, flexible and easy to implement. Independent control of the sources minimizes the complexity of the master controller. The intelligent controller is the brain of the system that decides the power flows and disconnects the sources that are not being used. Fig. 5.12 shows the algorithm that the controller follows. Decision making is done on two occasions: whether the battery would be included in the circuit, and if yes, then it decides the mode of operation of the bi-directional dc-dc converter. The sign of the P_{batt} is the variable used to decide whether the converter would operate in the buck mode or the boost mode. The dc link voltage is regulated by the inverter; so if there is a need to isolate the system from the grid, then the commanded power is forced to zero. It does not provide physical isolation.

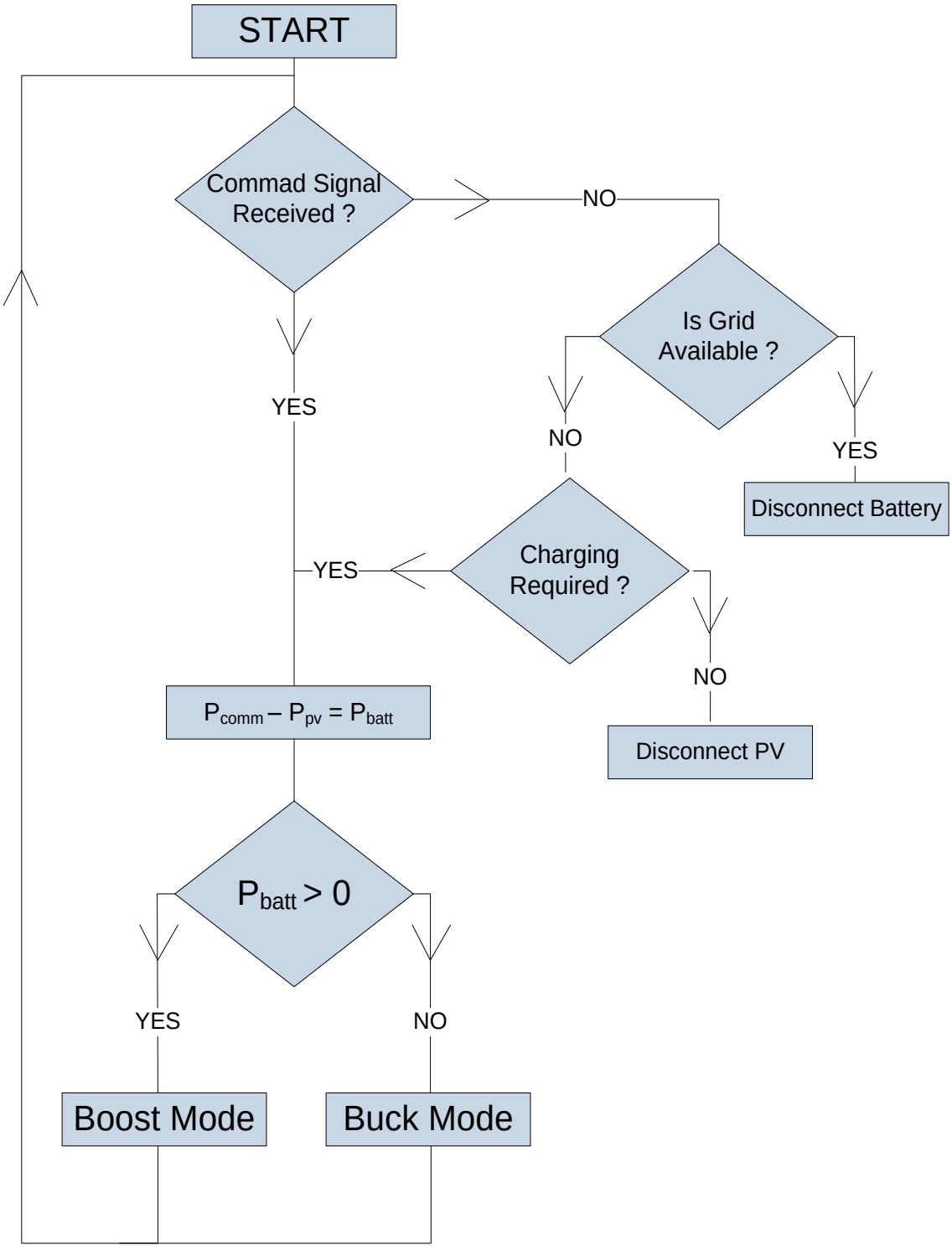

Figure 4.12 Intelligent controller algorithm

5. SIMULATION RESULTS

An analysis and study of the complete system is done under various scenarios. Each case simulation is done in Matlab/Simulink R2010a and PLECS [42].

The following are the scenarios for which the system was tested:

Case 1 – Power transfer from PV to grid with battery disconnected

Case 2 – Battery charging during daytime and night time

Case 3 – Active power transfer from grid and PV to the battery with reactive power support – down regulation

Case 4 – Active power transfer from PV and battery to the grid with reactive power support – up regulation

5.1 CASE 1: PV SUPPLIES GRID; NO REGULATION

Under the normal operating condition, i.e., when the system is not participating in regulation, the system is responsible for injecting all of the generated PV power into the grid at unity power factor. The battery is disconnected in this scenario. The boost converter connected to the PV array will track the maximum power, while the inverter regulates the DC link voltage to 400 V and transfers the ac power to the grid.

Fig. 5.1 shows the PV power output for variable insolation levels. One can see that for decreased insolation levels, the PV power drops to zero for an instant before attaining its steady state value. This is a mathematical problem of MATLAB PV model and does not necessarily happen in real life. Fig. 5.2 shows the RMS power measured at the AC side. It is clear that the controller effectively tracks the array power and transfers the ac power into the grid.

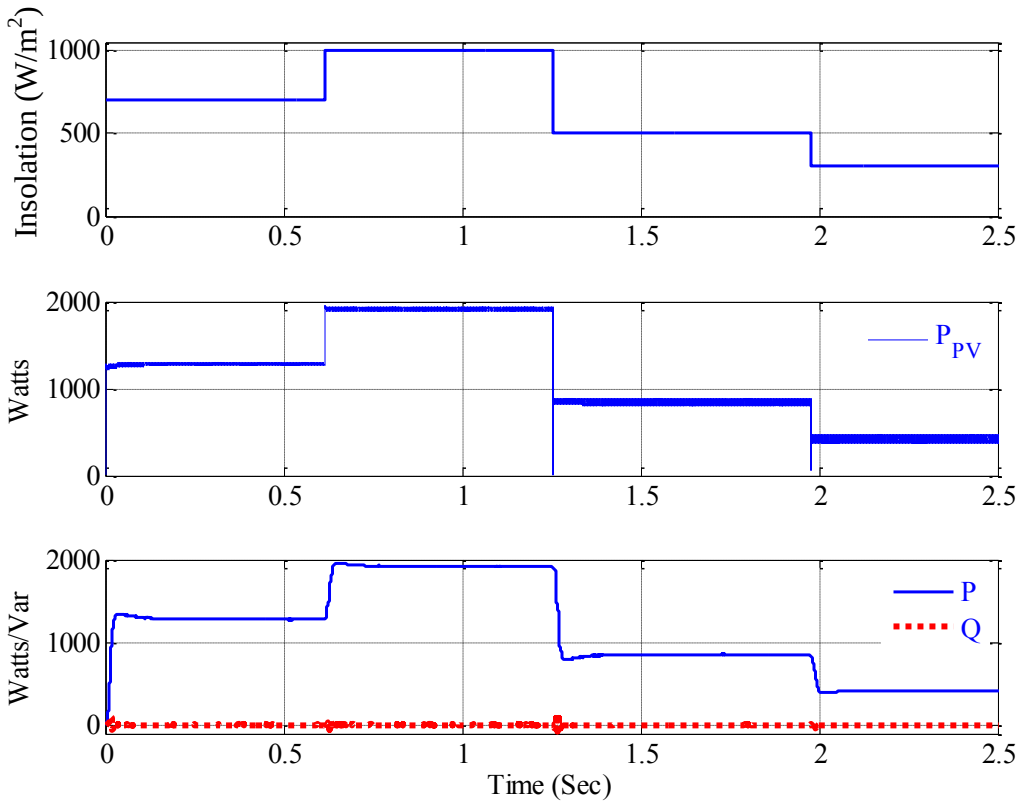

Figure 5.1 PV array output for variable insolation on the ac side.

5.2 CASE 2: BATTERY CHARGING FROM PV/GRID

The system is tested under the scenario where the battery has been depleted, and therefore, there is a need to charge the battery. Most utility companies who buy power back from PV producing customers pay only a fraction of what they charge for selling energy to the customer [43]. If there is PV power available such as during daylight hours, it is reasonable to utilize it to charge the battery. In such a scenario, an intelligent controller senses the battery SOC and, based on the maximum charging current of the battery; it generates a reference current for the bi-directional dc-dc converter.

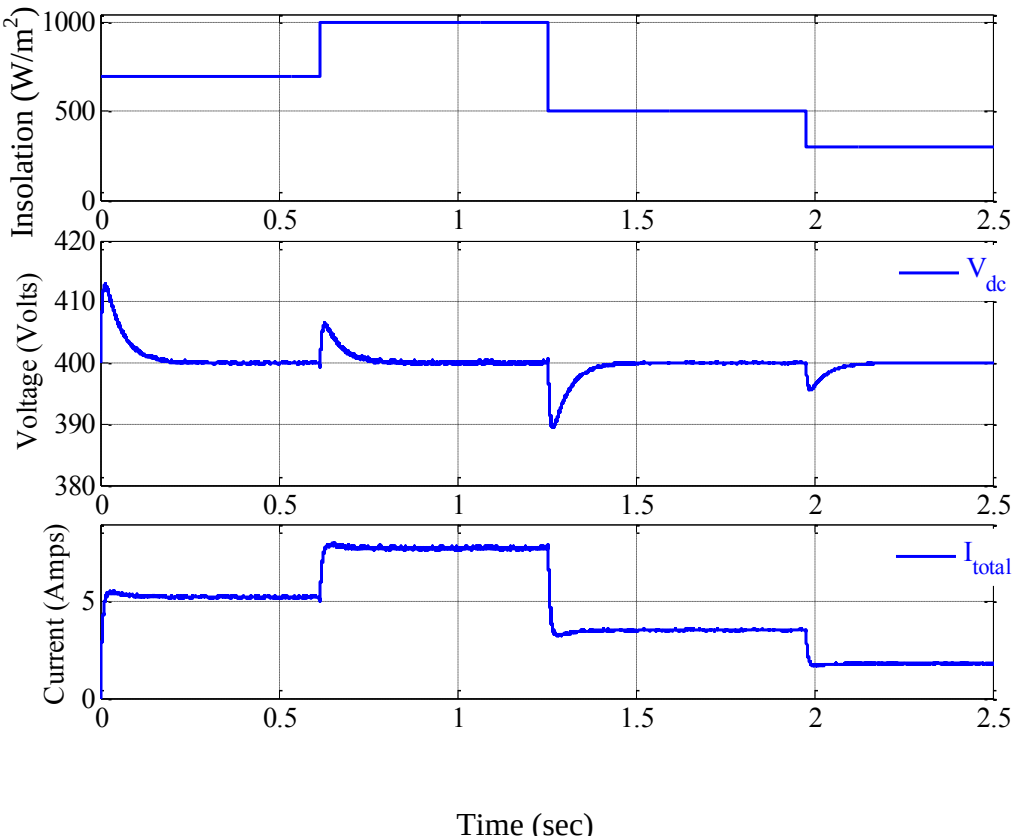

Figure 5.2 DC link voltage and current from PI compensator

Fig. 5.3 shows the PV power available under two different insolation levels. The controller sends the entire PV power available into the battery and, therefore, the active and reactive power on the AC side is zero. If the power required for charging is less than the power produced by the PV, then inverter will transfer the extra energy to the grid. Negative power for 'P_{batt}' means that the battery is absorbing power.

Figure 5.4 shows the current through the inductor. One can see that as commanded power changes, the average current going into the battery also changes. This is one of the advantages of the proposed control scheme.

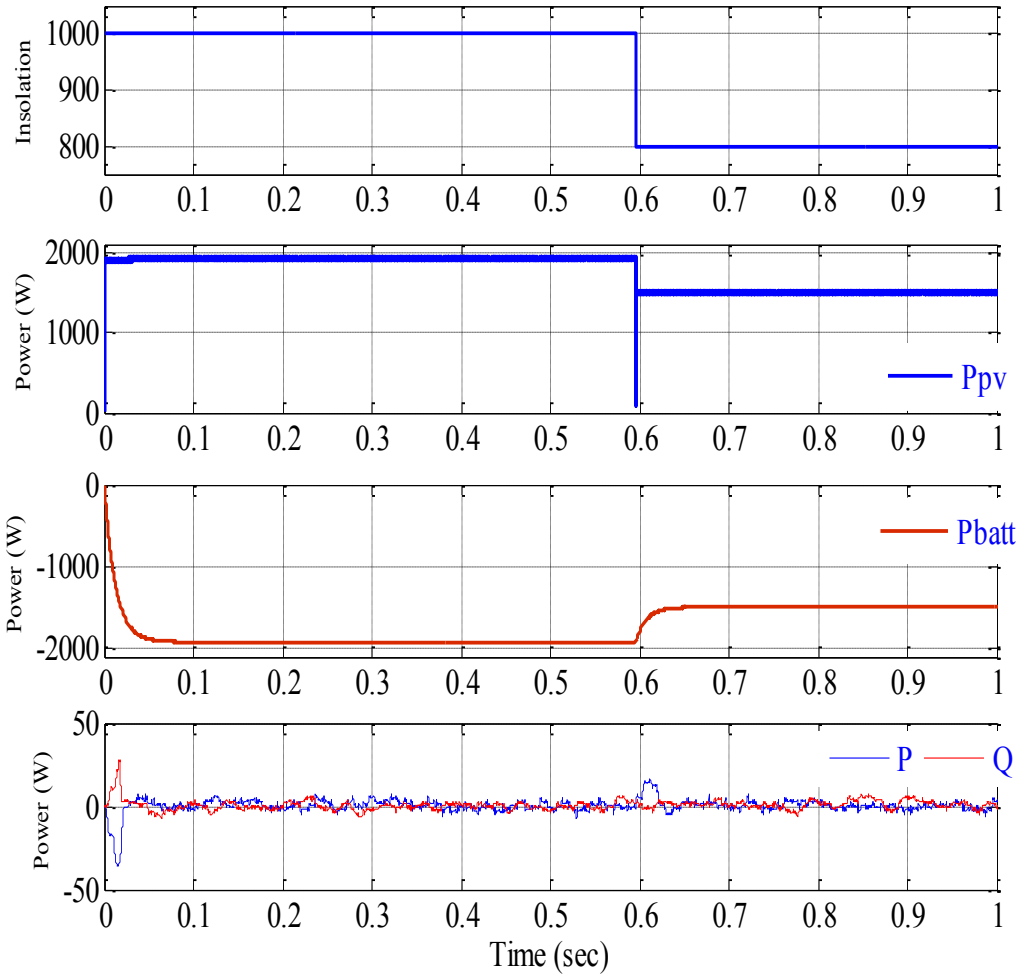

Figure 5.3 Battery charging with available power from the PV array

The current going into the battery may be controlled and, thus, the battery can be operated in either trickle charge or fast charge mode. If the PV power is not available i.e. during night time or poor weather conditions, then the battery will be charged with power received from the grid. Again, based on the battery conditions, the correct amount of power can be commanded from the grid, and the three phase bridge will work as an active rectifier as shown in Fig. 5.5. Fig. 5.6 shows the current going into the battery and one can see that controller is providing very fast tracking of the commanded current.

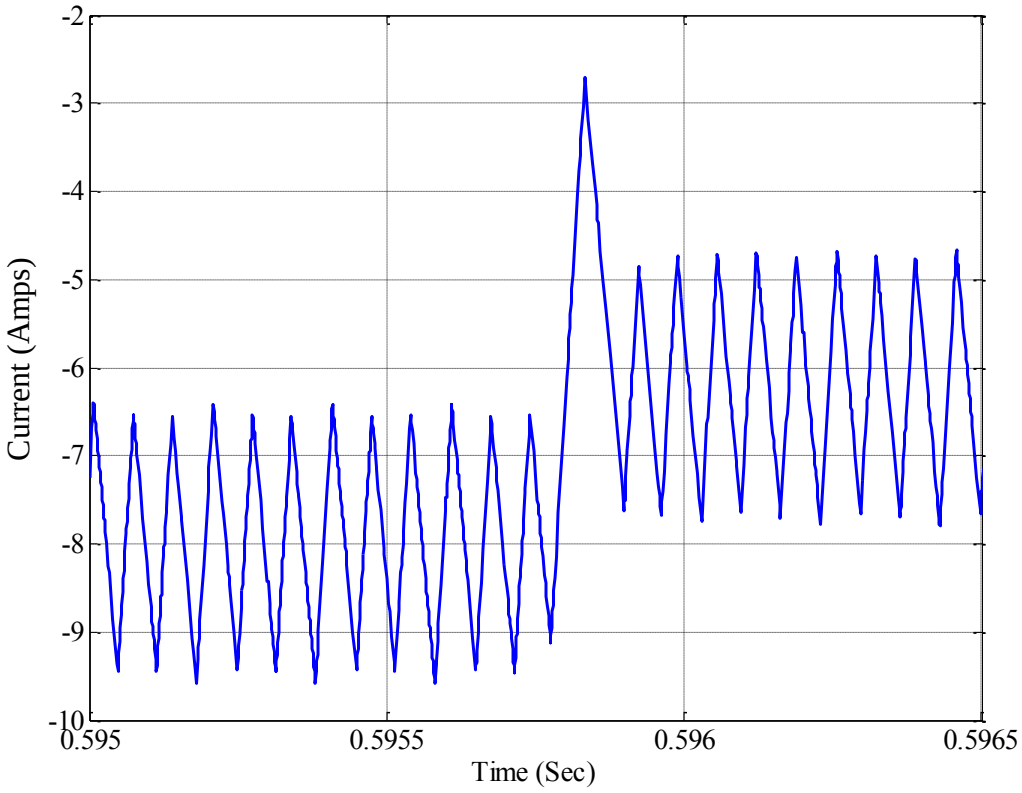

Figure 5.4 Current through the inductor of the bi-directional DC-DC converter

5.3 CASE 3: DOWN REGULATION

Down regulation will be defined as the case when the grid has some amount of excess generation which has caused the system frequency to increase above 60 Hz, and therefore, it wants to shed its excess generation. The PV/battery system is simulated under this scenario where there is a need to absorb a certain amount of active power from the grid. The bottom half of Fig. 5.7 represents the signal received from the grid operator commanding the PV/battery system to switch modes in order to fulfill its demand.

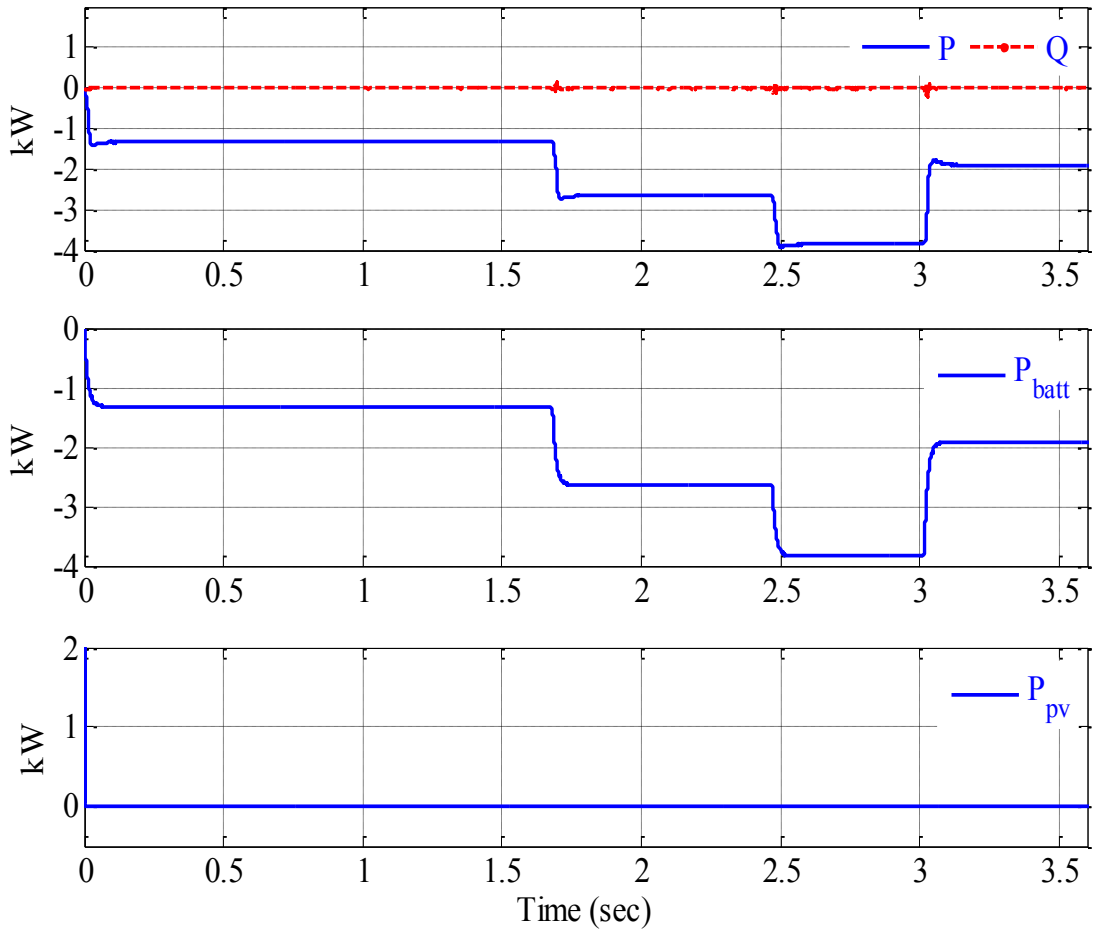

Figure 5.5 Battery charging with power commanded from the Grid

The commanded signal indicates that there is a need for different levels of active power. The bottom half of Fig. 5.7 is the RMS power observed at the grid side. It can be seen that the controller is very fast in following the commanded signal.

Fig. 5.8 shows the power on the dc side of the system. The three phase bridge is operating as an active rectifier and the bi-directional dc-dc converter connected between the dc bus and the battery is operating in the buck mode.

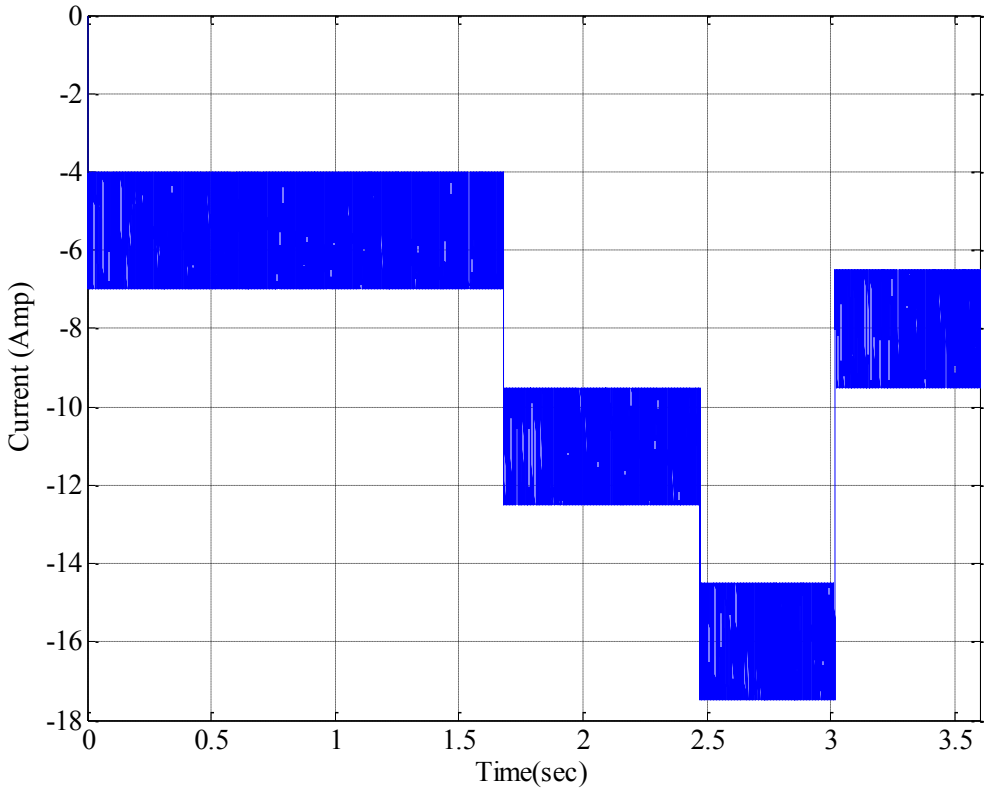

Figure 5.6 Current through the inductor of the bi-directional dc-dc converter while charging the battery with power commanded from the grid.

The power coming from the PV and the grid is being absorbed by the battery. At t = 2.25 sec, there appears a change in insolation from 800 W/m^2 to 600 W/m^2 and one can see that the converter injects less power into the battery. Fig. 5.9 shows the SOC and the current going into the battery.

Fig. 5.10 shows the dc link voltage throughout the down regulation period. At t = 2.53 sec, there is a large perturbation in active power demand from 10,000 W to 5,000 W.

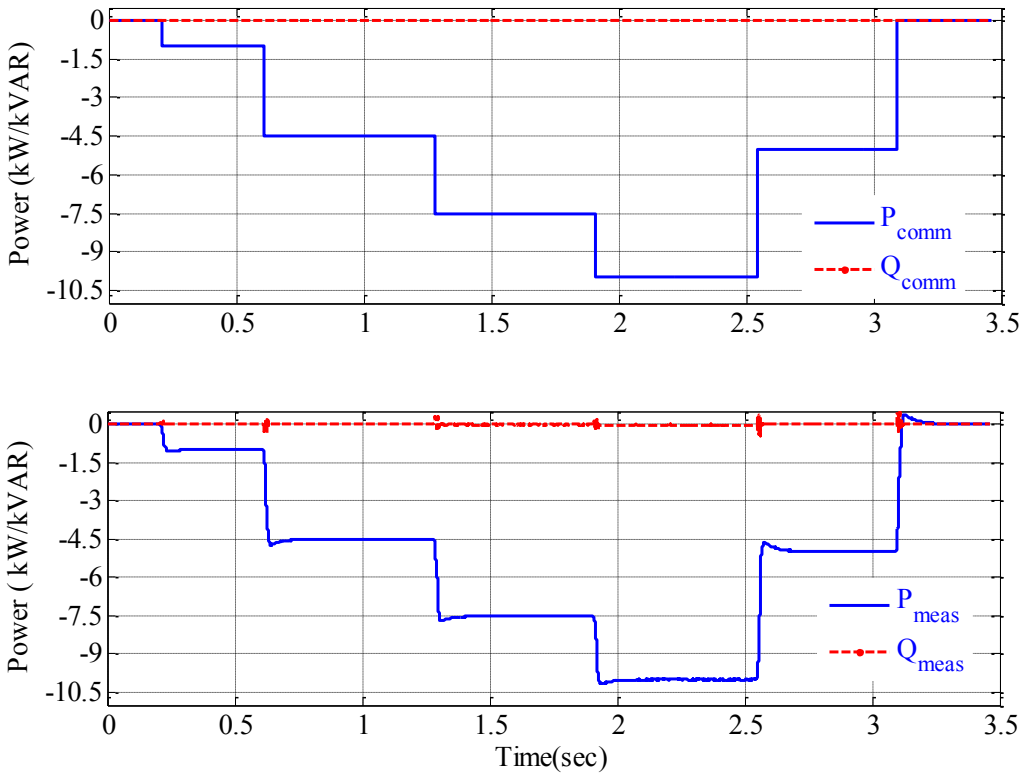

Figure 5.7 Power measured on the ac side for case 3

The spike in the dc link voltage is a result of this perturbation in demand. The maximum amount of overshoot observed is 12.5 % which is a reasonable margin since the usual practice is to keep the overshoot under 20%. The settling time is observed to be 0.2 sec.

Fig. 5.11 shows the currents observed on the grid side during the down regulation. Currents are almost sinusoidal with a negligible amount of distortion. The filter inductor placed at the output of the inverter is 8 mH this inductor is responsible for the smooth sine wave at the output. Harmonics in the current are a function of filter response and switching frequency of the inverter.

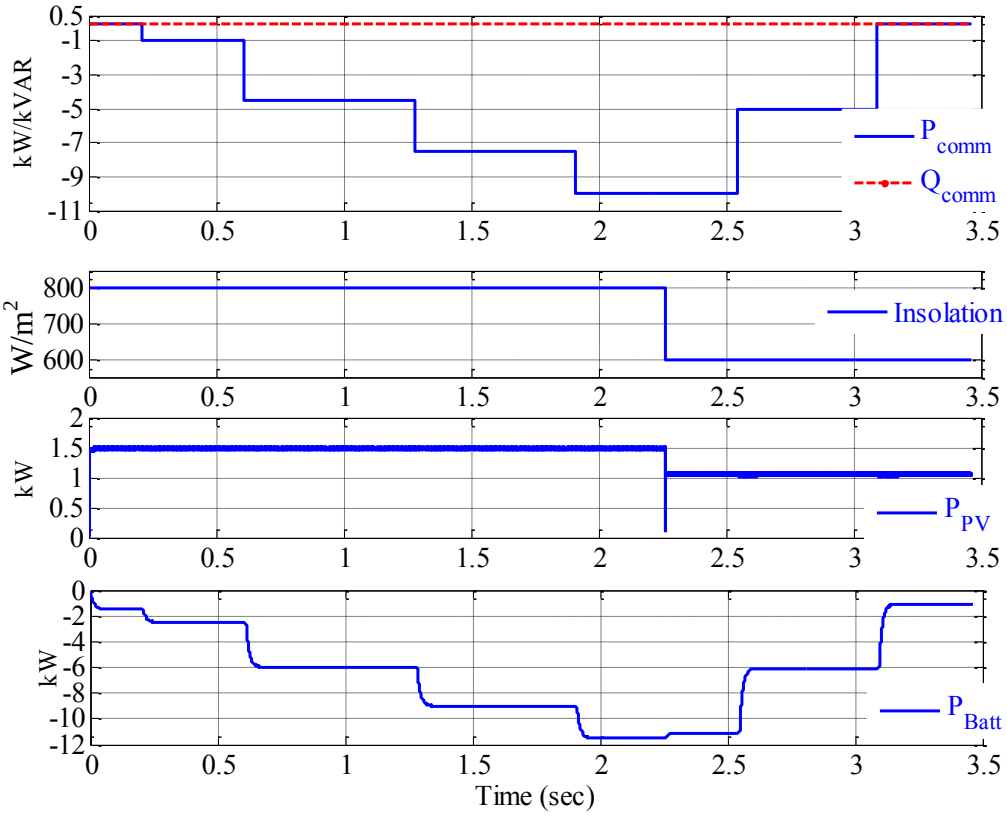

Figure 5.8 Power at the dc side for case 3

For low power applications, MOSFETs are available which can be used at high switching frequencies. IGBTs, on the other hand, limit the switching frequency. In the delta modulation scheme, the switching frequency is variable but the maximum switching frequency can be controlled.

Further tests are done to observe the performance of the system in absorbing and injecting reactive vars. The PV array is producing 1000 watts and the active power demanded by the grid is -1500 watts thus battery is receiving 2500 watts.

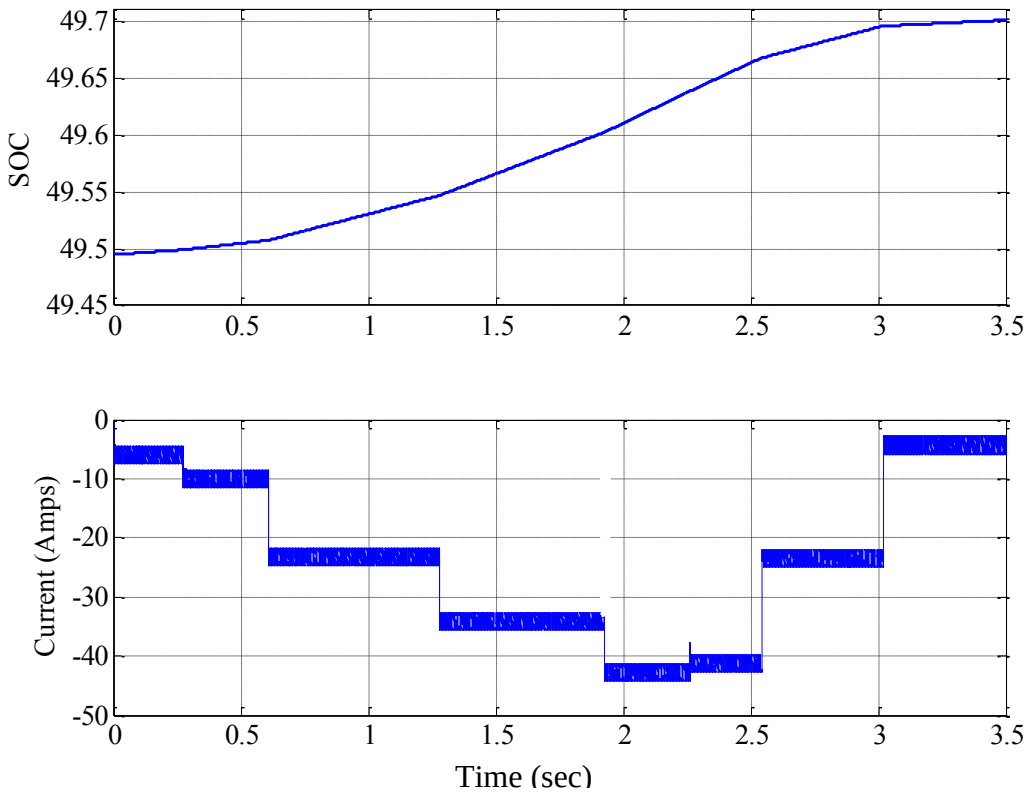

Figure 5.9 SOC and battery current for case 3

As shown in Fig. 5.12, at t = 0.5 sec, a command signal is received to absorb reactive power from the grid, and at t = 2 sec, the inverter injects reactive power into the grid. One interesting point to note is that although the inverter is injecting reactive power, it has no effect on the power on the dc side because of the presence of the capacitor at the input of the inverter; this may be observed in Fig. 5.13. The average dc current going into the battery is only a function of the active power. The DC link capacitor is responsible for absorbing or producing the commanded reactive power.

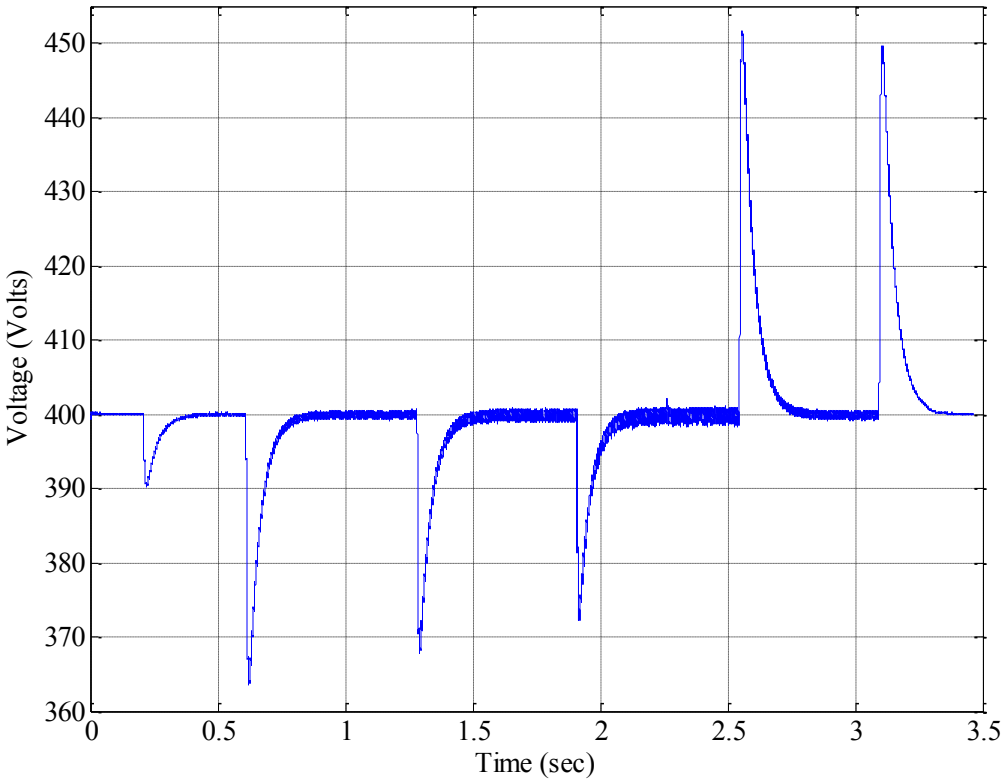

Figure 5.10 DC link voltage for case 3

Between time t=1.25 sec and t=2 sec, system is handling 1200 W active power and 6000 Vars reactive power. The operating kVA of the system is therefore 6.11 kVA, which is below the inverter rating of 10 kVA. The reactive power that a system can deliver is mainly dependent on the size of the inverter. The size of the inverter imposes restrictions on the reactive power capability because of the current and voltage stress limitations of the switches. It also depends on the reactance of the filter placed at the output terminal of the inverter and the DC bus voltage. However, they can be designed carefully in order to utilize the inverter fully.

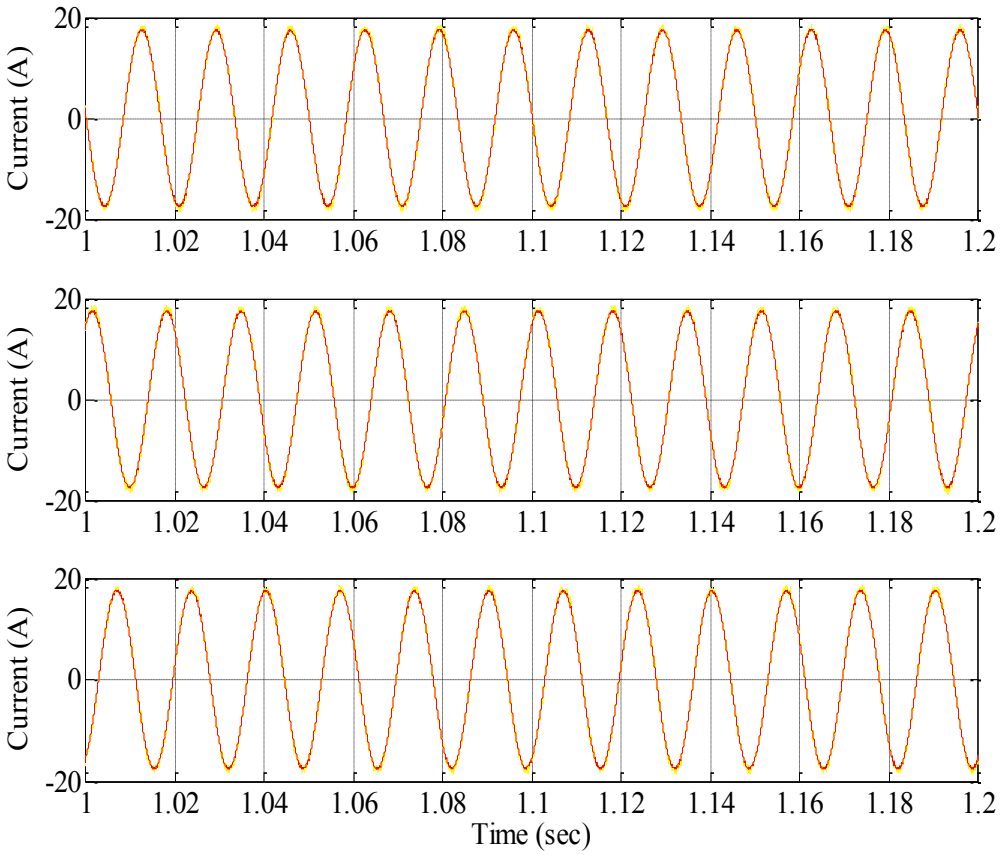

Figure 5.11 AC currents at the grid side for case 3

5.4 CASE 4: UP REGULATION

Up regulation will be defined as the case when the grid has generation shortage which has caused the system frequency to drop below 60 Hz, and therefore, it wants to purchase generation from one community-based PV system. During the period of up regulation, the PV/battery system is responsible for injecting active power into the grid. As shown in Fig. 5.14, the system responds very quickly to the commanded signal received from the grid fulfilling variable amounts of active and reactive powers demanded.

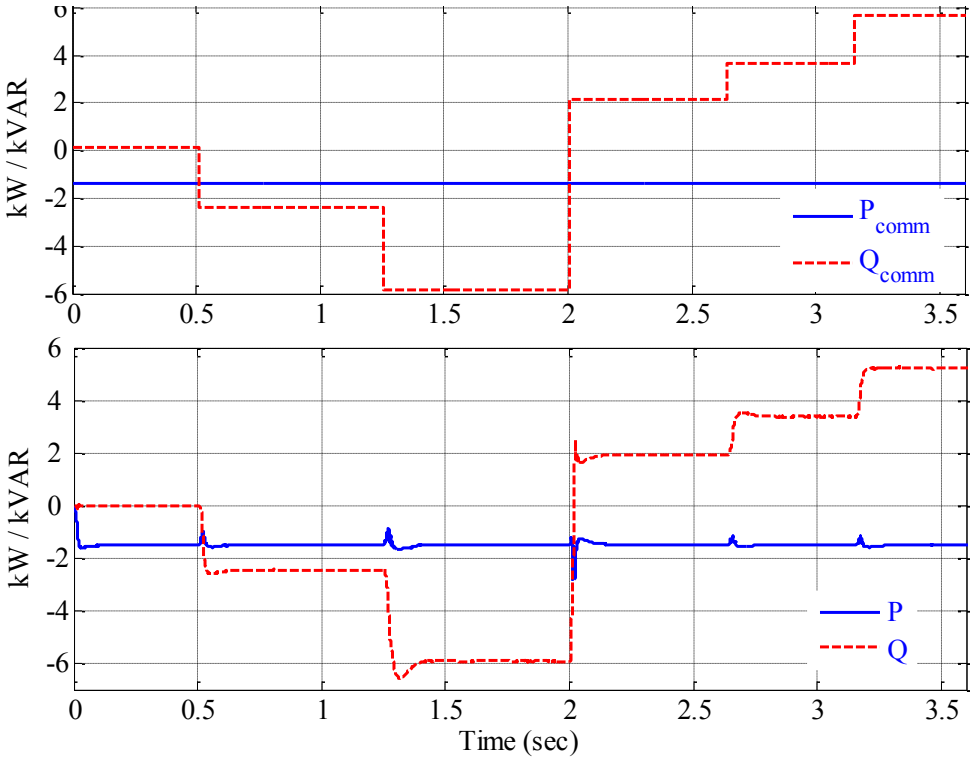

Figure 5.12 Providing voltage support to the grid for case 3

This scenario tests the system's capability to change the mode of operation of the bi-directional DC-DC converter. One can see from Fig. 5.15 that initially, the commanded signal is for 1000 Watts demanded by the grid, and the PV power output is approximately 1900 Watts. In this case, the inverter injects 1000 Watts into the grid and the bi-directional DC-DC converter operates in the buck mode, i.e., charging the battery with 900 Watts of power. At t=0.4 sec, the commanded signal changes to 3000 Watts and there is a need for extra power from battery. So, the dc-dc converter changes its mode from buck to boost and supplies the additional power demand.

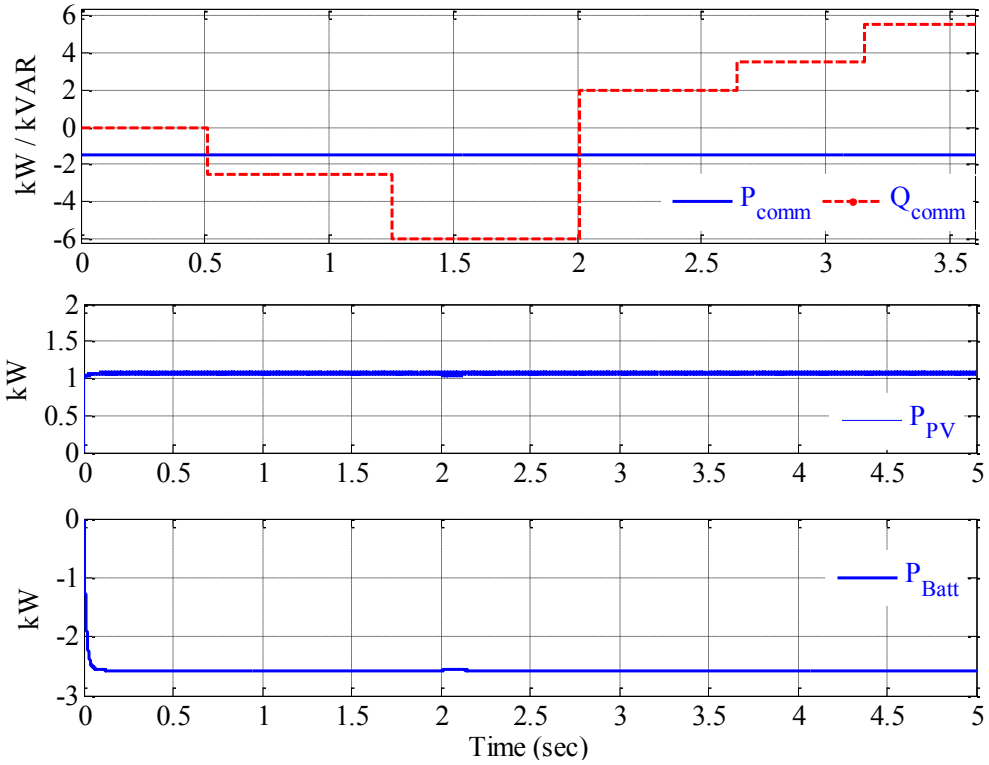

Figure 5.13 Power on the dc side during reactive power support for case 3

Fig. 5.16 shows a snapshot of the per phase voltage and currents on the AC side during the time frame where the system receives the command for reactive power support. At t=2.17 sec, the commanded signal is to absorb 2000 Vars from the grid. This is in addition to the demand for 2500 Watts of active power. One can see that delta modulation method forces a smooth transition smoothly and the current starts to lead the voltage by 38.65° after t=2.17 sec.

The amount of regulation that the system is providing is just a part of the overall frequency and voltage regulation requirement. It is assumed that there are other DGs

which are also under frequency and voltage control and are responsive to grid commands in order to provide a viable regulation amount that the grid might need.

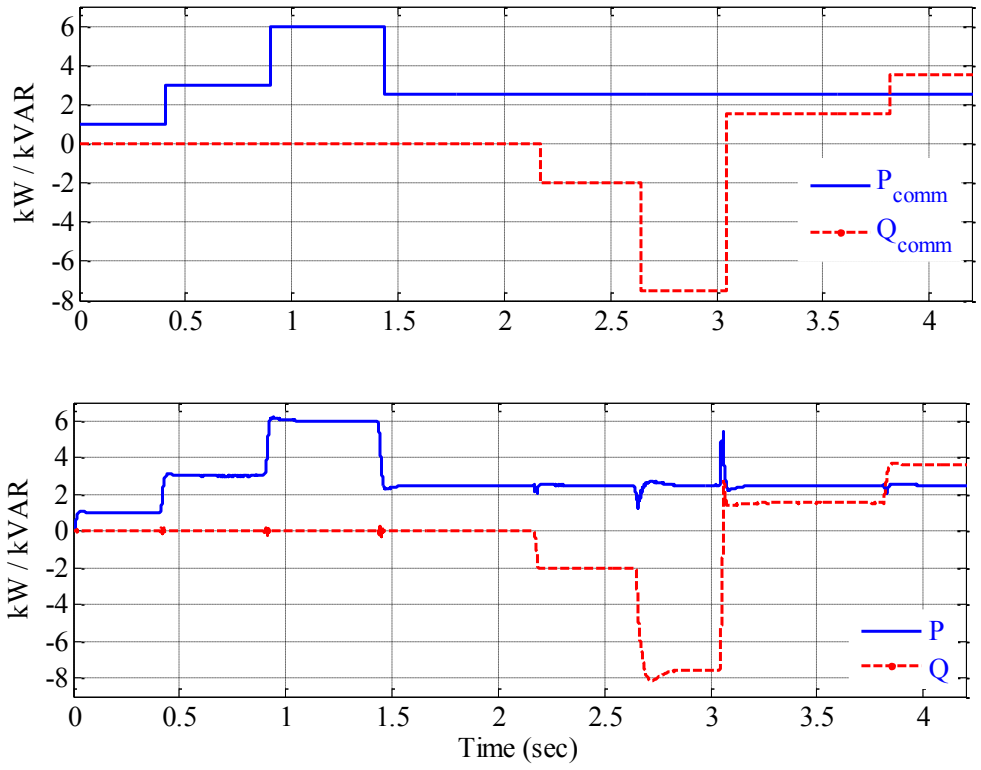

Figure 5.14 Up regulation with both active and reactive power commands

To summarize, the system is capable of operating under many scenarios and these are listed in Table 5.1. By means of proper switching, all the energy sources can be isolated from one another. All modes of operation, except Mode 1, are possible even when PV is

not available. All the results shown are based on the assumption that the grid is commanding the power only if the PV/battery system is capable of providing it.

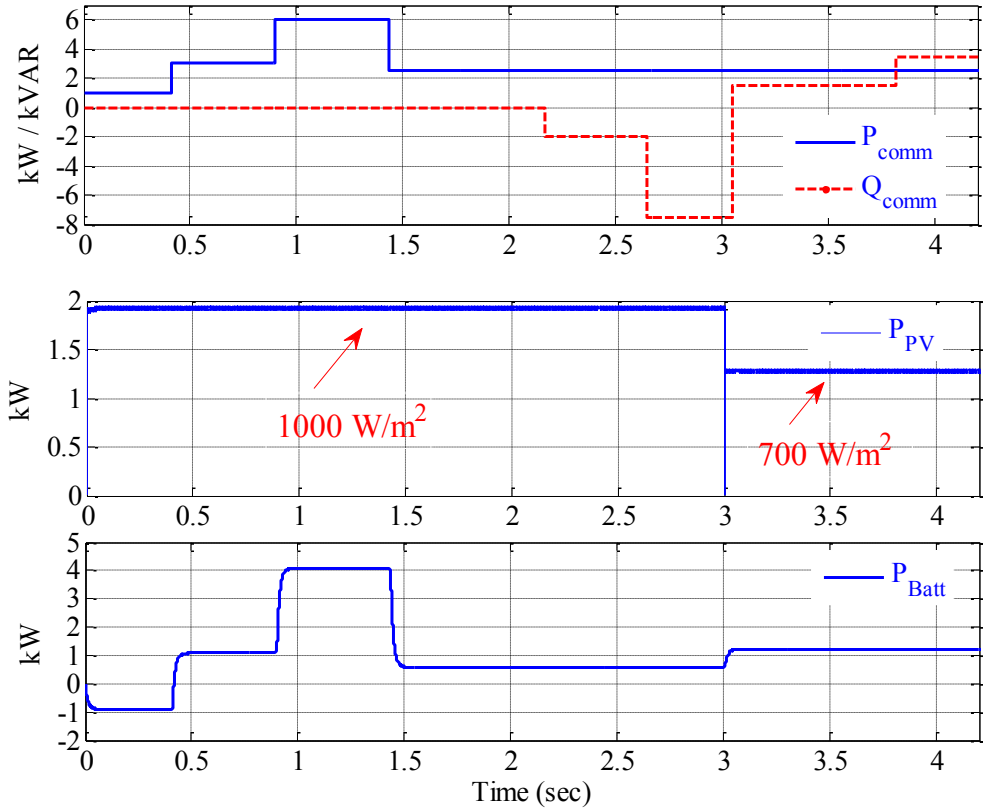

Figure 5.15 Power at the dc side for case 4

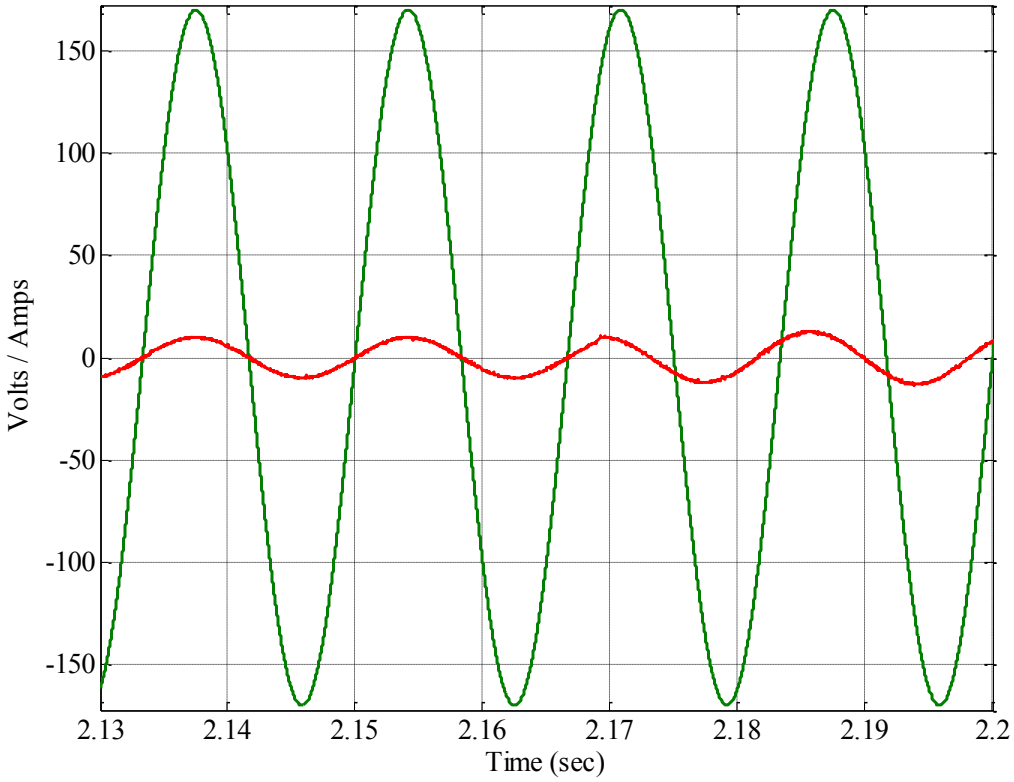

Figure 5.16 Per phase voltage and current for case 4

Table 5.1 Power Flow under various scenarios

	Mode of operation	**Power Flow**
1.	No regulation signal	PV to Grid
2.	Battery Charging	PV to Battery (Day time) Grid to Battery (Night time)
3.	Down regulation	(PV + Grid) to Battery
4.	Up regulation	(Batt + PV) to Grid

6. CONCLUSION AND FUTURE WORK

A new technique to implement grid frequency and voltage support capability in a solar photovoltaic power plant in the framework of the Smart Grid is presented. This method allows effective control over active and reactive power available from the system. A system comprising of a 2 kW PV array, 2.64 kWh Li-ion battery with bi-directional dc-dc converter, three phase inverter and the grid was modeled, and simulated in the MATLAB Simulink environment. This system is only a building block in an overall scheme where many of such systems may be made available to respond to grid requirements. The battery was selected to increase the reliability and flexibility of the system. A two-way communication link is essential to update the grid operator regarding the status of the active and reactive power capability of the system. This helps the operation in asking for specific amounts of P and Q support from each renewable energy facility at a given time. Results show that based on the commanded signals, the PV plant can respond quickly and can participate in regulation. The control techniques adopted are simple, autonomous and easy to implement. To test the system's capability, four different scenarios were tested. The first case is where there is no need for regulation and the system merely injects the PV energy into the grid with the battery disconnected. The second case shows the system's ability to charge the battery from either the PV energy or the grid based on the availability of either resource. The third case shows the system's ability to fulfill commanded active and reactive power demands during down regulation mode, i.e. absorbing power from the grid. The fourth case simulates the up regulation mode where the system injects the commanded active power into the grid with reactive power support.

The control technique adopted is not limited to only PV. Other intermittent sources with their own control can also be integrated into the system either on the AC or the DC side. The system is scalable. One more advantage of such power management scheme is that the battery current is controlled providing freedom to the user to handle the battery based on its chemistry and requirements.

One of the most important factors in the up- and down- regulation is the size of the system. Depending on the size of the feeder, market economics, geographical conditions, etc., the PV plant and the battery storage can be sized in such a way to have the highest impact. The proposed technique is most useful if used as a community-based PV system. Providing regulation support based on the economic price signal can lower the investment payback period of the PV system.

6.1 RECOMMENDATIONS FOR FUTURE WORK

The next step is to check the feasibility of the scheme in a hardware implementation. The choice of the battery technology will have a significant impact on the effectiveness of the scheme. In addition, there are other challenges such as depth of discharge, life cycle expectancy, self discharge rate and installation cost. A comparative study is required to determine the most effective battery technology to be used to serve the purpose. Further research is required in the area of regulation market, standards and grid codes. The inverter plays a critical role in the regulation scheme since it handles both the active and the reactive power flow. A study is required in developing the criteria for selecting the proper inverter size for such applications.

APPENDIX A.

PV PANEL DATASHEET

GE-PV 200 W module

Peak Power (Wp)	Watts	200
Max. power voltage (Vmp)	Volts	26.3
Max. Power Current (Imp)	Amps	7.6
Open Circuit Voltage (Voc)	Volts	32.9
Short Circuit Current (Isc)	Apms	8.1
Short Circuit Temp. Coefficient	$mA/^0C$	5.6
Open Circuit Voltage Coefficient	$V/^0C$	-0.12

APPENDIX B.

MAXIMUM POWER POINT TRACKING ALGORITHM

dp/dv algorithm

```
% Maximum power tracking using dp/dv method

function y = del(u)        % Call function for Vref

global del;

global v;

global Im;

global Pm; % initial value for the sensed power, Pm = 0 (initially)

global Vm;

E=(u(1)*((u(2)-Im)/(u(1)-Vm)))+u(2); % Error in the value dP/dV

if E>0.02 && abs(Vm-u(1))>0.01

v=u(1)+0.5*abs(Vm-u(1))/2 + 0.025*E; % if slope is positive increase

Reference Voltage

elseif E<0.02 && abs(Vm-u(1))>0.01

v=u(1)-0.5*abs(Vm-u(1))/2+ 0.025*E; % if slope is negative decrease

Reference Voltage


else

v= u(1);

end

abs(Vm-u(1));

Vm=v;

Im=u(2);  % Update the Pm, Vm and Im variables

y=v;
```

APPENDIX C.

SYSTEM PARAMETERS

PV panel rating = 200 W

No. of panels in series = 5

No. of panels in parallel = 2

PV array rating = 2000 W

V_{mpp} = 131.5 volts (for STC)

V_{grid} L-L_{rms} = 208 Volts

V_{dc} steady state = 400 volts

DC link capacitance = 1000 µF

V_{batt} = 240 Volts

I_{batt} nominal = 11 Ah

Nominal battery capacity = 2.64 kWh

Filter inductance = 8 mH

Inductance of boost converter (PV) – 5 mH

Inductance on boost converter (battery) – 2.16 mH

BIBLIOGRAPHY

[1] James G. Cupp and Mike E. Beehler "Implementing Smartgrid communications," Burns and McDonnell Tech brief 2008 [Online] Available: http://www.smartgridnews.com/artman/uploads/1/article-smartgrid-part2-084.pdf, [Accessed: APR 20,2011]

[2] Denis Lenardic, "Large Scale Photovoltaic Power plants", May 31,2010 [Online] Available: http://www.pvresources.com/en/top50pv.php, [Accessed: June 06,2010]

[3] Lazarewicz, M.L. and Rojas, A.,"Grid frequency regulation by recycling electrical energy in flywheels," Proc. IEEE Power Engineering Society General Meeting, June 2004, Vol.2, pp.2038-2042

[4] Huajun Yu, Junmin Pan, and An Xiang, "A multi-function grid-connected PV system with reactive power compensation for the grid," Solar energy, 79, (2005), pp101-106

[5] Brendan J. Kirby, "Frequency Regulation Basics and Trends", Oak Ridge National Laboratory Report number ORNL/TM-2004/291, December 2004.

[6] Xiaoyan Yu; Tolbert, L.M.; "Ancillary services provided from DER with power electronics interface," IEEE Power Engineering Society General Meeting, 2006.

[7] Martin Braun, "TECHNOLOGICAL CONTROL CAPABILITIES OF DER TO PROVIDE FUTURE ANCILLARY SERVICES," Division Engineering and Power Electronics, Institut fuer Solare Energieversorgungstechnik (ISET)

[8] E. Hirst, B. Kirby, "Creating Competitive Markets for Ancillary Services" ORNL/CON-448, Oak Ridge National Laboratory, Oak Ridge, TN, October 1997.

[9] "Power systems services provided by DER", Mar 10,2010[online] Available: http://derlab.eu/public/media/pdf/docs/Power_system_services_provided_by_DER_units.pdf, [Accessed: May 10,2011]

[10] Chuang, A.S.; Schwaegerl, C., "Ancillary services for renewable integration," Integration of Wide-Scale Renewable Resources Into the Power Delivery System, CIGRE/IEEE PES Joint Symposium, July 2009.

[11] J. B. Campbell, T. J. King, B. Ozpineci, D. T. Rizy, L. M. Tolbert, Y. Xu, UTK and X. Yu, UTK, "ANCILLARY SERVICES PROVIDED FROM DER", Oak Ridge National Lab, Report No. ORNL/TM-2005/263 Dec 2005

[12] Tomás Gómez1, Chris Marnay, Afzal Siddiqui, Lucy Liew, and Mark Khavkin, "Ancillary Services Markets in California", Environmental Energy Technologies Division, Ernest Orlando Lawrence Berkeley National Laboratory, Report No. LBNL-43986, July 1999.

[13] Slootweg, H.; , "Smart Grids - the future or fantasy?," Smart Metering - Making It Happen, 2009 IET , Feb. 2009

[14] Bevrani, H.; Ghosh, A.; Ledwich, G.; , "Renewable energy sources and frequency regulation: survey and new perspectives," Renewable Power Generation, IET, pp.438-457, September 2010

[15] Faria, P., Vale, Z., Soares, J., Khodr, H. and Canizes, B., "ANN based day-ahead ancillary services forecast for electricity market simulation," 15th IEEE Mediterranean Electrotechnical Conference, April,2010

[16] P. Faria, Z. Vale, J. Soares, H. Khodr, "ANN based Day-Ahead Spinning Reserve Forecast for Electricity Market Simulation", The 15th International Conference on Intelligent System Applications to Power Systems (ISAP2009), Curitiba, Brazil, November 2009

[17] John D. Kueck, Brendan J. Kirby, Leon M. Tolbert, and D. Tom Rizy, "Voltage regulation - Tapping Distributed Energy Resources", Public Utilities Fortnightly, Sept. 2004 [Online] Available: http://www.pur.com/pubs/4427.cfm, [Accessed]: May05,2011

[18] Yan XU, D. Tom RIZY, Fangxing LI, and John D. KUECK, "Dynamic Voltage Regulation Using Distributed Energy Resources", 19th International Conference on Electrical Distribution (CIRED), May 07

[19] Renewable Portfolio Standards Fact Sheet, U.S. Environmental Protection Agency, [Online] Available: http://www.epa.gov/chp/state-policy/renewable_fs.html, [Accessed]: May 12,2011

[20] Miller, N. and Ye, Z. “Report on Distributed Generation Penetration Study,” Report NREL/SR-560-34715, NREL – National Renewable Energy Laboratory, U.S. Dept. of Energy, Golden, Colorado, August 2003.

[21] Raugei M., Frankl P. Life cycle impacts and costs of photovoltaic systems: Current state of the art and future outlooks, Energy, March 2009.

[22] Liu, Y.; Bebic, J.; Kroposki, B.; de Bedout, J.; Ren, W.; , "Distribution System Voltage Performance Analysis for High-Penetration PV," IEEE Energy 2030 Conference, Nov. 2008

[23] Karlynn S. Cory, Jason Coughlin and Charles Coggeshall, “Solar Photovoltaic Financing: Deployment on Public Property by State and Local Governments”, Strategic Energy Analysis and Applications Center, National Renewable Energy Laboratory, Aug. 2008 [online] Available: http://www1.eere.energy.gov/wip/solutioncenter/pdfs/tap_webinar_20080813.pdf, [Accessed]: Apr 05,2011

[24] Electricity Advisory Committee, “Bottling electricity: storage as a strategic tool for managing variability and capacity concerns in the modern grid”, Dec. 2008 [Online] Available: http://www.oe.energy.gov/DocumentsandMedia/final-energy-storage_12-16-08.pdf, [Accessed]: Apr, 22, 2011

[25] Smith, S.C, Sen, P.K., and Kroposki, B., "Advancement of energy storage devices and applications in electrical power system," IEEE Power and Energy Society General Meeting - Conversion and Delivery of Electrical Energy in the 21st Century, July 2008.

[26] Vartanian, C.; , "Grid stability battery systems for renewable energy success," Energy Conversion Congress and Exposition (ECCE), 2010 IEEE, Sept. 2010

[27] Gregory G. Stamas, “The Promise of Grid Storage: Applications, Regulation, and Revenue-Maximizing Policies for Energy Arbitrage”, Department of Operations Research and Financial Engineering, Princeton University, April 2010

[28] Stratis Tapanlis and Michael Wollny, “Advanced Active And Reactive Power Control For Mini Grids”, World Climate & Energy Event, Mar. 2009

[29] Borlea, I.,Kilyeni, St., Barbulescu, C. and Cristian, D., "Substation ancillary services fuel cell power supply. Part 1. Solution overview," Computational Cybernetics and Technical Informatics (ICCC-CONTI), 2010 International Joint Conference, May 2010

[30] Lu, D., and Francois, B., "Strategic framework of an energy management of a microgrid with a photovoltaic-based active generator," Advanced Electromechanical Motion Systems & Electric Drives Joint Symposium, 8th International Symposium, July 2009

[31] Liming Liu, Yan Zhou and Hui Li, "Coordinated active and reactive power management implementation based on dual-stage PLL method for grid-connected PV system with battery," Energy Conversion Congress and Exposition (ECCE), Sept. 2010

[32] Sun, K., Zhang, L., Xing, Y. and Guerrero, J., "A Distributed Control Strategy based on DC Bus Signaling for Modular Photovoltaic Generation Systems with Battery Energy Storage," IEEE Transactions on Power Electronics, 2009

[33] Tina, G.M., and Pappalardo, F., "Grid-connected photovoltaic system with battery storage system into market perspective," IEEE PES/IAS Conference, Sustainable Alternative Energy (SAE), Sept. 2009

[34] E. Liu and J. Bebic, “Distribution system voltage performance analysis for high-penetration photovoltaics,” NREL/SR-581-42298, Tech. Rep., 2008.[Online].Available:http://www1.eere.energy.gov/solar/pdfs/42298.pdf,[Accessed: MAR 15,2011]

[35] Pappu, V.A.K.; Chowdhury, B.H.; Bhatt, R.; , "Implementing frequency regulation capability in a solar photovoltaic power plant," North American Power Symposium (NAPS), 2010 , vol., no., pp.1-6, 26-28 Sept. 2010

[36] M. Francisco L. González, “Model of Photovoltaic Module in Matlab,” Latin American Congress of Students of Electrical Engineering, Electronic and Computation, 2005.

[37] GE PV 200W Solar module characteristics, Available: http://www.powerupco.com/panels/ge.php, [Accessed: MAR 01,2011]

[38] Open Source PV model, University of Colorado Boulder [Online] Available: http://ecee.colorado.edu/~ecen2060/energyprogram.html, [Accessed]: Jan. 2010

[39] Esram, T.; Chapman, P.L.; , "Comparison of Photovoltaic Array Maximum Power Point Tracking Techniques," IEEE Transactions on Energy Conversion, June 2007

[40] Tremblay, O., Dessaint, L.-A., and Dekkiche, A.-I., "A Generic Battery Model for the Dynamic Simulation of Hybrid Electric Vehicles," IEEE Vehicle Power and Propulsion Conference, Sept. 2007

[41] Paul C. Krause, Oleg Wasynczuk and Scott D. Sudhoff, "Analysis of Electric Machinery and Drive Systems", second edition, p.512

[42] PLECS Blockset - http://www.plexim.com/, [Accessed]: APR 23,2011

[43] Ameren UE, [Online] http://www.ameren.com/sites/aue/Rates/Documents/umbe1Mrtppo.pdf, [Accessed]: May 11, 2011

VITA

Ravi Bhatt was born on June 18, 1986 in Mumbai, Maharashtra, India. He completed his Bachelor of Engineering (B.E.) in Electrical Engineering from Fr. C. Rodrigues Institute of Technology, Navi Mumbai, India in May 2009 and Diploma in Electrical Engineering from Shri Bhagubhai Mafatlal polytechnic, Mumbai, India in May 2006. He started his Master of Science program in Electrical Engineering at Missouri University of Science and Technology in August 2009 and will receive his Master's degree in Aug 2011. Prior to joining the Master's program he has worked as an Engineering Intern at TATA Power Co. Ltd. and SIEMENS Ltd. His research interests include integration of renewable energy sources and modeling and control of power electronic converters.